

25 Group, Permian Rotliegend and Zechstein Groups and Triassic Skagerrak Formation) extend
26 further than previously supposed, and therefore the presence of possible sub-volcanic
27 reservoir and source rock units may have been overlooked within the triple junction of the
28 Central North Sea.

29 **Introduction**

30 The Middle Jurassic Rattray Volcanic Province (RVP) lies at the triple junction of the North
31 Sea rift system at the intersection of the Viking Graben, Central Graben and Outer Moray
32 Firth (Fig. 1). These volcanic rocks – variously referred to in literature as the Forties Volcanics
33 (Woodhall & Knox 1979), the Forties-Piper basalt field (Dixon *et al.* 1981), the Forties Igneous
34 Province (Ritchie *et al.* 1988) and the Rattray Formation (Deegan & Scull 1977) – were
35 discovered by the Forties Field discovery well (21/10-1) in 1970 which unexpectedly drilled
36 through >700 m of volcanic rocks beneath the Upper Cretaceous Chalk Group. The volcanic
37 sequence has since been penetrated by >200 hydrocarbon exploration and appraisal wells and
38 is comprised of basaltic lavas and volcanoclastic sedimentary units. The RVP covers an area of
39 ~7,400 km², with the thickest drilled volcanic sequence reaching ~1.5 km thick on the Buchan-
40 Glenn Horst.

41 Despite its position at the centre of the prospective rift system, little research has
42 focussed on the volcanism in the last 25 years, due to low perceived hydrocarbon potential
43 of the interval. The majority of research on the Rattray Volcanics was conducted in the late
44 1970s to early 1990s, focussing on analysis of core data such as lithological descriptions
45 (Howitt *et al.* 1975; Woodhall & Knox 1979), geochemical analysis (Gibb & Kanaris-Sotiriou
46 1976; Dixon *et al.* 1981; Fall *et al.* 1982; Latin *et al.* 1990a; Latin & Waters 1992), and
47 radiometric dating (Ritchie *et al.* 1988). The broader significance of the relationship of the
48 Rattray Volcanics at the rift triple junction to the tectonic evolution of the North Sea has also

49 been the subject of much discussion (Dixon *et al.* 1981) with some authors favouring a passive
50 rift model of melt in areas of greatest stretching (Latin *et al.* 1990a and 1990b; Latin & Waters
51 1991 and 1992) and others favouring an active rift model of thermal anomaly-induced rifting
52 (Underhill & Partington 1993). While the volcanics have been studied extensively at both
53 core-scale and regional-scale, relatively few studies have used seismic reflection data to
54 interrogate their nature and origin (e.g. Smith & Ritchie 1993; Stewart 1999). 3D seismic
55 reflection data can be used to map magma plumbing pathways, extrusion points and lava flows
56 in subsurface volcanic fields, allowing eruption histories and styles of volcanic provinces to be
57 investigated (Planke *et al.* 2005; Magee *et al.* 2014; McLean *et al.* 2017; Schofield *et al.* 2017a;
58 Reynolds *et al.* 2018; Hardman *et al.* 2018).

59 Here we use regional 3D seismic datasets to re-evaluate the architecture of the RVP
60 and provide new insights into the nature of the volcanic eruptions at the centre of the North
61 Sea trilete rift. The currently widely-accepted model (Husmo *et al.* 2002; Johnson *et al.* 2005)
62 for the RVP invokes eruption from three potential central volcanoes (Smith & Ritchie 1993),
63 termed the Glenn, Ivanhoe and Fisher Bank Volcanic Centres. We present evidence indicating
64 that the lavas were extruded in a series of fissure eruptions from linear vents and small
65 associated volcanic edifices rather than central point sources, and identify a major fissure
66 system in the RVP. We observe no evidence in seismic and well data to support the premise
67 of three central volcanoes sourcing Rattray volcanism. We suggest the lack of large central
68 volcanoes and associated shallow magma chambers beneath the Rattray Volcanics indicates
69 unexplored pre-volcanic petroleum systems may be present in the North Sea triple junction
70 area.

71 **Stratigraphy**

72 The Rattray Volcanics Member comprises part of the Middle Jurassic Pentland Formation (Fig.
73 2) and is coeval with the Ron Volcanics Member ~150 km to the south in the West Central
74 Graben (Richards *et al.* 1993). The origin of the Ron Volcanics Member is not studied in detail
75 in this paper. Lavas and volcanoclastic sedimentary rocks of the Rattray Volcanics Member are
76 interbedded with siliciclastic fluvio-deltaic sedimentary rocks (Richards *et al.* 1993) around the
77 fringes of the lava field. The Pentland Formation is dated as Bajocian-Bathonian from sparse
78 biostratigraphy data including long ranging miospores (Howitt *et al.* 1975), giving an age range
79 of 170.3 ± 1.4 Ma – 166.1 ± 1.2 Ma for the intercalated fluvio-deltaic sedimentary rocks on the
80 current chronostratigraphic timescale (Gradstein *et al.* 2012; Cohen *et al.* 2013). Radiometric
81 dating of the Rattray Volcanics Member using ^{40}Ar - ^{39}Ar dating indicated a likely magmatic age
82 of 153 ± 4 Ma - 148 ± 2 Ma (Ritchie *et al.* 1988), during the Kimmeridgian-Tithonian (Gradstein
83 *et al.* 2012; Cohen *et al.* 2013), contradicting the biostratigraphic ages from the interbedded
84 sedimentary rocks. Although the absolute age of eruption of the Rattray Volcanics Member is
85 inconclusive, the volcanics are generally presumed to have been erupted in the Bajocian-
86 Bathonian to Callovian (~170 Ma - 163.5 ± 1.0 Ma; Howitt *et al.* 1975; Underhill 1998; Husmo
87 *et al.* 2002).

88 While Pentland Formation siliciclastics are present beneath the volcanics in some wells
89 (e.g. 15/13-1 (Howitt *et al.* 1975)), the Rattray Volcanics Member usually sits unconformably
90 over a varied subcrop of Triassic and older rocks, with Lower Jurassic strata absent across
91 most of the triple junction area. This stratigraphic gap is known as the 'Mid-Cimmerian' or
92 'Intra-Aalenian' unconformity and is presumed to be the result of regional doming in the late
93 Toarcian-Aalenian (~182-170 Ma), which caused widespread subaerial erosion of Lower
94 Jurassic and uppermost Triassic strata across the Central North Sea (Underhill & Partington
95 1993). The presence of Late Jurassic marine sedimentary rocks overlying the Rattray Volcanics
96 Member indicates post-volcanic transgression occurred, likely associated with the deflation

97 and collapse of the dome (Underhill & Partington 1993). Transgression established shoreface
98 and marine shelf conditions over the fringes of the RVP in the Oxfordian and deposited some
99 of the major reservoirs in the Central North Sea, e.g. the Piper Formation sandstones in the
100 Outer Moray Firth. The stratigraphic position of the RVP indicates the eruption occurred
101 after the regional uplift in the latest Lower Jurassic–earliest Middle Jurassic (Underhill &
102 Partington 1993) and before the main phase of extension which formed the deep grabens of
103 the North Sea rift system in the Kimmeridgian-Tithonian of the Late Jurassic (Fraser *et al.*
104 2002).

105 **Previous Work: current understanding of the Rattray Volcanics Member**

106 ***Rattray lithologies***

107 Detailed lithological descriptions and geochemical analyses of the Rattray volcanic rocks can
108 be found in Howitt *et al.* (1975), Gibb & Kanaris-Sotiriou (1976), Woodhall & Knox (1979),
109 Fall *et al.* (1982), Latin *et al.* (1990a) and Latin & Waters (1992). The Rattray Volcanics Member
110 is dominated by silica undersaturated alkali olivine basaltic lava flows (Howitt *et al.* 1975;
111 Woodhall & Knox; 1979; Fall *et al.* 1982). The lavas are extensively weathered indicating
112 subaerial eruption and erosion (Gibb & Kanaris-Sotiriou 1976; Woodhall & Knox 1979).
113 Examples of subaqueous eruption have not previously been reported, though, if present, likely
114 occurred in fluvial and lacustrine settings in a broadly terrestrial environment (Latin *et al.*
115 1990a). The proportion of volcanoclastic sedimentary rocks increases towards the fringes of
116 the volcanic province (Howitt *et al.* 1975; Woodhall & Knox 1979). The volcanoclastics are
117 generally reworked and often incorporated into the interfingering Pentland Formation fluvio-
118 deltaic sedimentary rocks (Latin *et al.* 1990a). Small localised intrusions are present within and
119 beneath the lava pile (Howitt *et al.* 1975; Gibb & Kanaris-Sotiriou 1976; Fall *et al.* 1982; Ritchie
120 *et al.* 1988).

121 ***Proposed eruption mechanisms for the Rattray Volcanics***

122 Multiple different eruption styles and source areas have been proposed for the RVP including
123 extrusive vents (Howitt *et al.* 1975), fissure volcanism (Woodhall & Knox 1979), central
124 volcanoes (Smith & Ritchie 1993) and maar-diatremes (Stewart 1999).

125 *Extrusive vents*

126 Howitt *et al.* (1975) suggested three possible central extrusive vents trending from east to
127 west across the centre of the RVP in areas of increased drilled volcanic thicknesses and
128 positive aeromagnetic anomalies. The proposed vents are approximately aligned with the
129 Witch Ground Graben. Howitt *et al.* (1975) found no evidence of large scale intrusive bodies
130 associated with the magmatism and suggested that upwelling of the basaltic magma likely
131 occurred during the rifting of the Witch Ground Graben, exploiting pre-existing weaknesses
132 in the crust.

133 *Fissure volcanism*

134 Fissure volcanism involves the repeated effusion of low viscosity basaltic magma from a series
135 of linear fissure vents without a large-scale centralised volcanic vent system (Walker 1995).
136 Fissure vents are the surface expression of deep, narrow feeder dykes which feed the surface
137 volcanism from lower crustal magma reservoirs (Gudmundsson 1987), >20km depth
138 (Thordarson & Larsen 2007). Woodhall & Knox (1979) suggested the Rattray basalts were
139 erupted during repeated periods of fissure volcanism, citing a lack of evidence for suites of
140 intrusions and associated vent structures.

141 *Central volcanoes*

142 Central volcanoes have a sub-circular vent structure, commonly erupting both silicic and mafic
143 magmas (Walker 1971), and have a large plutonic intrusive complex beneath the core of the
144 structure (Walker 1995) forming the magma chamber for the volcano. Eroded roots of central
145 volcanoes are often observed onshore as large granitic and gabbroic plutons, e.g. the Skye and
146 Mull Central Complexes (Emeleus & Bell 2005), representing solidified magma chambers
147 (Walker 2000). Central volcanoes are usually associated with large sub-circular magnetic and
148 gravity anomalies as seen in the West of Scotland igneous complexes (Emeleus & Bell 2005),
149 offshore West of Britain in the Rockall Basin (Archer *et al.* 2005; Schofield *et al.* 2017b) and
150 Faroe-Shetland Basin (Chalmers & Western 1979; Jolley & Bell 2002). Smith & Ritchie (1993)
151 used seismic data, volcanic well thicknesses and magnetic anomaly data to suggest the Rattray
152 Volcanics were erupted from three central volcanoes: the Glenn Volcanic Centre on the
153 Buchan-Glenn Horst, the Fisher Bank Volcanic Centre in the Fisher Bank Basin, and the
154 postulated Ivanhoe Volcanic Centre in the Outer Moray Firth (Fig.1). This model is currently
155 the widely accepted eruption mechanism for the RVP (Husmo *et al.* 2002; Johnson *et al.* 2005).

156 *Maar-Diatremes*

157 Maars are volcanic craters, fed by pipes called diatremes, associated with the explosive
158 interaction of magma with shallow groundwater (Lorenz 1986; Stewart 1999). Stewart (1999)
159 interpreted four circular down-thrown fault blocks in the RVP on the southern slope of the
160 Renee Ridge affecting the Triassic and older stratigraphy as maar craters. These potential
161 maars are outwith the 3D seismic surveys used in this current study (Fig.3).

162 **Data & Methodology**

163 ***Seismic and Geophysical Data***

164 This study uses two 3D seismic reflection surveys from the Central North Sea – the PGS 3D
165 Central North Sea MegaSurveyPlus (MSP) and the PGS 3D North Sea MegaSurvey (MS) which
166 extend to ~6-7 seconds two-way-time (s TWT). The surveys cover an extensive area across
167 the North Sea; this study utilises the northern ~10,000 km² of the MSP and ~8,600 km² of the
168 MS covering areas of the RVP outwith the MSP (Fig.3a). The data are displayed in the time
169 domain where a downwards increase in acoustic impedance ('hard kick') corresponds to a
170 negative amplitude reflection (displayed in blue) (Fig.3b), and a downwards decrease in
171 acoustic impedance ('soft kick') corresponds to a positive amplitude reflection (displayed in
172 red). The vertical resolution ($\lambda/4$ (Kallweit & Wood 1982)) of the seismic data within the
173 subaerial Rattray lava package is calculated using an internal velocity of ~5504 m.s⁻¹ (calculated
174 from well 15/24b-3 depth ~3313m) with a dominant frequency in MSP seismic data of 24 Hz;
175 a lava thickness of ~57 m is required for an individual flow to be fully resolvable. Nexen's
176 AM852D1009 2D survey is used to aid interpretation in a gap between the MS and MSP 3D
177 data in the south of Block 15/23 (Fig.3). The vertical resolution of the 2D survey for subaerial
178 lavas, using an internal velocity of ~5504m.s⁻¹ with a dominant frequency of 18 Hz, is ~76 m.

179 Digital Magnetic Anomaly data at 1:50,000 for Central North Sea Quads 6 through to
180 39 is provided by the British Geological Survey (BGS). Magnetic anomaly data outside of this
181 area, as well as offshore gravity anomaly data, is accessed on the BGS Offshore Index.
182 Formation depths from well data were used to guide seismic interpretation with wells (Fig.3)
183 accessed on the UK Oil and Gas Database.

184 ***Wireline facies interpretation***

185 Detailed volcanic wireline facies analysis was undertaken in several wells across the RVP.
186 Digital log curves used for facies interpretation include gamma ray, deep resistivity, density,
187 neutron, and acoustic travel time curves. Volcanic facies analysis in this study has been guided

188 by the wireline facies interpretation and methodologies of Planke (1994), Nelson *et al.* (2009),
189 Watton *et al.* (2014), Millett *et al.* (2016a) and Watson *et al.* (2017) and was checked against
190 Rattray core facies where available. Typical examples of the petrophysical characteristics of
191 the main basaltic volcanic facies in the Rattray Volcanics Member are shown in Figure 4. All
192 basaltic facies produce low gamma values, typically between 15-60 API, due to the low
193 proportion of potassic minerals. Tabular basaltic lava flows – formed by thick, individual flow
194 units – produce blocky log motifs of high resistivity (>50-200 ohm.m), high density (~2.7-2.9
195 g.cm⁻³) and fast internal velocity (~40-60 $\mu\text{s.ft}^{-1}$ or ~5.1-7.6 km.s⁻¹). Compound basaltic lava
196 flows – formed by multiple stacked thin flow units – exhibit more serrated log motifs than
197 tabular lavas and typically have slightly lower densities and acoustic velocities (Nelson *et al.*
198 2009) due to the high proportion of vesicular crust in compound flows.

199 Hyaloclastite is formed by the quenching and fragmentation of lava during interaction
200 with water (Watton *et al.* 2014) and is identified in the RVP in this study. Subaqueous basalt
201 typically has lower resistivity, density and acoustic velocity than subaerial basalt due to
202 increased fracturing and higher porosity (Bartetzko *et al.* 2005). Hyaloclastite log profiles can
203 be highly variable dependent on its physical properties and composition (Nelson *et al.* 2009;
204 Watton *et al.* 2014; Millett *et al.* 2016a). Hyaloclastite has high neutron porosity values (40-60
205 pu in the Rattray Volcanics) due to high vesicularity and clay-bound water (Planke 1994;
206 Bartetzko *et al.* 2005; Watton *et al.* 2014). Basaltic volcanoclastic sedimentary rocks exhibit
207 low gamma, medium-high resistivity (~10-20 ohm.m), are acoustically fast but slower than
208 subaerial lavas (~60-80 $\mu\text{s.ft}^{-1}$) and are less dense than subaerial lavas (~2.3-2.5 g.cm⁻³). Basaltic
209 volcanoclastics exhibit high neutron values due to clay-bound water, and produce a
210 characteristic density-neutron response similar to shales, with the neutron on the left of the
211 density curve (Watson *et al.* 2017).

212 **Subsurface mapping of the Rattray Volcanics**

213 The depth to the top of the Pentland Formation is highly variable across the triple junction
214 area (Fig. 5) due to faulting during the major Late Jurassic rifting event. The Rattray Volcanics
215 Member is at its shallowest depth on the footwalls of Late Jurassic fault blocks (e.g. Piper Shelf,
216 Renee Ridge) at 2-2.4 s TWT (approximately 2.3-2.8 km vertical depth below the sea surface).
217 The deepest burial of the volcanics is in the downthrown structures of the Witch Ground
218 Graben and Fisher Bank Basin, where the top of the Pentland Formation is at depths of 4.4-
219 4.9 s TWT (~5.6-6.2 km).

220 Figure 1b shows the thickness of the Pentland Formation around the triple junction
221 area. Most wells stopped drilling within the volcanics without reaching the base of the Rattray
222 sequence. The thickness map is constructed from well thicknesses and seismic mapping of the
223 near top and base Pentland Formation surface. The Rattray Volcanics Member is thickest in
224 the Witch Ground Graben and Buchan-Glenn Horst, where it reaches thicknesses of ~1.3-
225 1.5 km (Fig.1b). The thickest drilled Rattray sequence is on the Buchan-Glenn Horst, with
226 ~1469m of volcanics penetrated in well 21/03b-3.

227 **Investigating source areas of Rattray volcanism**

228 Here we re-evaluate the architecture of the RVP using 3D seismic data to determine the type
229 of eruptions that sourced the Rattray volcanism.

230 ***Buchan-Glenn Horst***

231 The Buchan-Glenn Horst is the site of an elongate positive magnetic anomaly (200-250 nT),
232 ~25 km long and ~9 km wide, oriented WSW-ENE (Fig. 6a). The elongate shape of the
233 magnetic anomaly aligns with the shape of the uplifted horst block and is likely a response of

234 the dense basement and thick (~1.5 km) ridge of Rattray volcanic rock on the Buchan-Glenn
235 Horst.

236 *Seismic Line A-A': Buchan-Glenn Horst*

237 Figure 6b/c shows a seismic line running W-E across the Buchan-Glenn Horst. The Rattray
238 Volcanics Member forms a ridge of material ~0.45 s TWT (~1.2 km) thick across the Buchan-
239 Glenn Horst structure, above a thick (0.86 s TWT; ~2.1 km) siliciclastic sedimentary package,
240 likely comprising Devonian-Carboniferous Old Red Sandstone (ORS), with a thin (~24 m)
241 Permian carbonate package between the ORS and volcanics (21/03b-3 end-of-well report).
242 The ORS seismic reflections beneath the volcanic sequence are laterally continuous and can
243 be traced beneath the Rattray on the Buchan-Glenn Horst and into the adjacent basin (Fig.
244 6c(1)). A bright, discontinuous, discordant reflection is highlighted within the Rattray sequence
245 to the west of the Glenn anomaly peak (Fig. 6c(2)). Bright, discontinuous stratigraphically
246 concordant reflections are present within the ORS package (Fig. 6c(3)).

247 A thick (~0.45 s TWT/1.2 km) package of inclined seismic reflections (Fig. 6c(4)) is
248 observed within the volcanic sequence and appears to downlap the sub-Rattray sedimentary
249 sequence, dipping in a south-westerly direction. The inclined reflections appear to be
250 truncated at the Top Rattray surface (Fig. 6c(5)), possibly recording post-volcanic erosion in
251 this area. Similar packages of inclined seismic reflections are observed within the Rattray
252 Volcanics Member across the Buchan-Glenn Horst, Renee Ridge and extend into the Witch
253 Ground Graben to the north and Forties-Montrose High to the south.

254 *Seismic Line A-A' Interpretation*

255 We observe no evidence of large-scale volcanic vent structures in seismic data indicative of a
256 central volcano in the Buchan-Glenn Horst area. The bright, discontinuous reflections within

257 the volcanic and ORS packages likely represent igneous intrusions. A sill cross-cuts the Rattray
258 lava seismic reflections and is not observed to be feeding a volcanic vent or edifice (Fig. 6c(2)),
259 indicating that the intrusion occurred after the eruption of the majority of the lavas. While
260 sills are present on the Buchan-Glenn Horst structure (Ritchie *et al.* 1988), they are spatially
261 restricted and not mappable on seismic across a large area; there is no evidence on seismic
262 data for a kilometre-scale intrusive sill complex expected with central complex volcanism.

263 The inclined seismic reflections on the Buchan-Glenn Horst have previously been
264 interpreted as the depositional dips of lavas on the flanks of a central volcano (Smith & Ritchie
265 1993) or tectonically-induced dips (Stewart 1999). Inclined seismic reflections in volcanic
266 sequences can represent the presence of lava deltas, which form at the transition from
267 subaerial to subaqueous lava emplacement (Jones & Nelson 1970; Wright *et al.* 2012) when
268 lava builds out into a standing water body. Our re-evaluation of wireline volcanic facies in
269 nearby wells (e.g. 15/21-3 and 15/24b-3) indicates that thick (~70 m) hyaloclastite packages
270 are present in the Rattray Volcanics Member. We therefore suggest that the inclined seismic
271 reflections in Fig. 6c(4), while likely also affected by later tectonic rotation during Late Jurassic
272 extension, actually represent foresets of lava that built out in a standing water body forming
273 a hyaloclastite delta.

274 *Seismic Line B-B': Sub-vertical seismic discontinuities*

275 Seismic line B-B' from north to south across the Buchan-Glenn Horst shows a series of sub-
276 vertical discontinuities through the Rattray and older strata (Fig. 7). Each discontinuity is
277 represented by red-blue-red triplets of sub-vertical seismic reflections (Fig. 7a(1)). The
278 reflection triplets are ~0.4-1 km apart. These reflection triplets extend to depths of around 4
279 s TWT; below this discontinuities in the seismic continue in the same orientation and extend
280 towards the base of the seismic line, but do not extend above the Rattray sequence. The

281 discontinuities dip $\sim 65^\circ$ north-westwards, trend in a broadly WSW-ENE direction, and can
282 be mapped across numerous seismic lines across the central Rattray area on the Buchan-
283 Glenn Horst, reaching ~ 25 km in length.

284 *Seismic Line B-B' Interpretation*

285 We interpret the NW-dipping linear features as reflections caused by igneous dykes. Dykes
286 are rarely clearly imaged on seismic data due to their narrow width and near-vertical
287 structure. However, sub-vertical zones of seismic disturbance have been interpreted as
288 representative of igneous dykes in the Southern North Sea (Underhill 2009; Wall *et al.* 2010)
289 and offshore South Australia (Holford *et al.* 2017), and reflections from dykes have been
290 imaged offshore southern Norway (Phillips *et al.* 2017). The Rattray dykes would have been
291 near vertical at the time of emplacement; their current orientation of dipping $\sim 65^\circ$ to the
292 NW is presumably related to later tectonic movements, possibly regional tilting that occurred
293 across the triple junction area following Late Jurassic rifting (Stewart 1999). Rotation of the
294 dykes to approximately vertical re-instates the lavas across the area to sub-horizontal.

295 *Spectral Decomposition of Seismic Data*

296 A frequency decomposition flattened on the Top Rattray surface in the Buchan-Glenn Horst
297 area highlights a linear seismic discontinuity coincident with the position of the interpreted
298 dykes (Fig. 8a). The WSW-ENE linear feature is ~ 25 km long and < 800 m wide and has bright
299 areas extending NW and SE on either side. Five small circular features ~ 1 km in diameter are
300 aligned along the discontinuity. Four shorter (~ 2.5 - 8.5 km long) discontinuities are found ~ 1 -
301 7 km to the north and south of the main linear feature. These discontinuities variably trend
302 WSW-ENE and SW-NE and are less pronounced than the main feature.

303 *Spectral Decomposition Interpretation*

304 The dyke highlighted in Fig. 7b(1) is interpreted as having fed a ~25 km long linear volcanic
305 fissure system running WSW-ENE through the Buchan-Glenn Horst (Fig. 8b(1)), coincident
306 with the location and orientation of the positive magnetic anomaly. The linear nature of the
307 interpreted fissure system differs markedly from the curvilinear shape of the major post-
308 volcanic Late Jurassic fault planes (Fig. 8b(2)), an aspect also noted in seismically imaged dykes
309 offshore southern Australia (Holford *et al.* 2017). The other discontinuities (e.g. Fig. 8b(3))
310 likely represent other dykes in close proximity to the fissure – the dyke in Fig. 7b(2) is
311 coincident with the discontinuity in Fig. 8b(3). It is unclear whether these dykes fed surface
312 lavas, but if so they may represent minor fissure vents. Bright areas in the Top Rattray surface
313 are highlighted appearing to extend away from the fissure zone (Fig. 8b(4)). These bright zones
314 are interpreted as lava flows, similar to those mapped within the Palaeogene lava sequences
315 of the Faroe-Shetland Basin (Schofield & Jolley 2013; Hardman *et al.* 2018), extruded from the
316 fissure system. The five circular structures (Fig. 8b(5)) are positioned centrally along the
317 interpreted fissure system and appear to source some of the lava flows in the area. A flow
318 extending south-eastwards from the eastern end of the fissure system has a different internal
319 morphology to lava flows (Fig. 8b(6)). Whereas the lava flows are relatively smooth surfaces,
320 this area has thin internal striations across the surface, and is dimmer than the nearby lava
321 flows. This may represent an alluvial system made up of eroded volcanic debris generated by
322 flow through the channelised fissure system after eruption had ceased.

323 *Seismic Lines C-C' and D-D'*

324 Seismic cross-sections through two of the circular structures located on the fissure are shown
325 in Figure 9. Each structure has positive relief relative to the surrounding Top Rattray surface

326 with a central depression and directly overlies a narrow zone of chaotic seismic reflections
327 within the Rattray sequence.

328 *Seismic Lines C-C' & D-D' Interpretation*

329 The circular structures in Fig. 8/9 are interpreted as small volcanic vents on the fissure system.
330 Vent C-C' is steep and narrow with a high vent rim and narrow crater. It is ~200 m high and
331 ~800 m in diameter, with an aspect ratio of ~1:4, close to the typical aspect ratio of a cinder
332 cone (1:5, Heiken 1971). Vent D-D' is ~150 m high and ~1320 m across, giving an aspect ratio
333 of ~1:9, which is typical of a tuff cone (Heiken 1971). The deep, narrow zone of seismic
334 disturbance beneath vent D-D' is also similar to the described morphology of a maar-diatreme
335 structure (Stewart 1999). Small volcanic cones can build up along fissure vents due to fire-
336 fountaining of basaltic magma as it degasses during effusion from the fissure (Kereszturi &
337 Németh 2012; Reynolds *et al.* 2016 and references therein).

338 *Buchan-Glenn Horst Summary*

339 Multiple sub-vertical discontinuities through the volcanic sequence and underlying
340 stratigraphy, and terminating at the top Rattray surface, are visible across the Buchan-Glenn
341 Horst. These discontinuities are interpreted as feeder dykes sourcing the Rattray Volcanics
342 in a series of fissure eruptions. A modern-day analogue for the Buchan-Glenn Horst fissure
343 and associated volcanic edifices is the ~27 km-long Laki fissure system, known as Lakagígar, in
344 southern Iceland (Thordarson & Self 1993) (Fig.8c). The Laki fissure system comprises ten
345 individual fissures, ~1.6-5.1 km in length, aligned en-echelon in close proximity (Thordarsen
346 & Self 1993). The identification of a closely-spaced suite of multiple feeder dykes on the
347 Buchan-Glenn horst is interpreted as forming a similar structure of individual fissure vents
348 forming one large fissure system.

349 The Buchan-Glenn Horst is close to the source of the Rattray volcanism, as previously
350 noted (Smith & Ritchie 1993). However, despite the thick volcanic succession present, there
351 is no obvious large-scale central volcano in the Rattray succession nor identifiable sill or
352 plutonic complex observed in the Rattray subsurface in the Buchan-Glenn Horst area. We
353 suggest the evidence is indicative of a feeder dyke swarm across the Buchan-Glenn Horst
354 sourcing the Rattray Volcanics in a series of fissure eruptions, and propose the name the
355 Buchan-Glenn Fissure System.

356 ***Northern Witch Ground Graben***

357 A positive magnetic anomaly of magnitude ~ 320 nT is present across Blocks 15/22, 15/23 and
358 15/24, ~ 35 km east of the Halibut Horst (Fig. 10a). It stretches ~ 40 km NW-SE and ~ 20 km
359 NE-SW and covers an area of ~ 700 km². It reaches a magnitude of ~ 320 nT close to well
360 15/23b-14 (Fig. 10a). Smith & Ritchie (1993) postulated that this magnetic anomaly may
361 represent an eruptive centre in the RVP, the Ivanhoe Volcanic Centre, but did not identify
362 the nature of the magnetic anomaly using seismic data.

363 *Seismic Line E-E'*

364 The peak of the magnetic anomaly is situated in a gap between the MSP and MS 3D seismic
365 surveys, but is imaged in Nexen's AM852D1009 2D survey (Fig. 10). Around the peak of the
366 magnetic anomaly near well 15/23b-14 the Rattray Volcanics seismic package is composed of
367 relatively laterally continuous seismic reflections which can be traced northwards across the
368 Witch Ground Graben. The Top Rattray surface does not contain any prominent structures
369 with positive relief indicative of a volcanic vent or edifice, although post-volcanic erosion could
370 have removed such features.

371 The Rattray Volcanics Member is downthrown to the north by a normal fault. A Late
372 Jurassic syn-rift seismic package of laterally continuous reflections lies above the Rattray on
373 the downthrown side, reaching ~570 m in thickness. The Rattray Volcanics Member thins to
374 the north from ~800 m (~0.36s TWT) against the fault to ~419 m in well 15/23-1Z. The
375 seismic reflections beneath the Rattray sequence are unclear, but a Permian sequence can be
376 extrapolated from the well penetration 15/23-1Z.

377 *Seismic Line E-E' Interpretation*

378 We do not observe any large-scale vent indicative of a central volcano, nor any discordant
379 seismic reflections in the volcanic subsurface which could indicate an igneous plumbing
380 complex beneath the Rattray Volcanics Member. There is no positive evidence on available
381 seismic data supporting the interpretation of a central volcano associated with the Ivanhoe
382 magnetic anomaly.

383 *Volcanic Wireline Facies in the Northern Witch Ground Graben*

384 Wells in the northern Witch Ground Graben contain thick (up to 70 m) sequences of basaltic
385 hyaloclastite and tabular lava flows (individual flows reaching over 30 m thick) with
386 volcanoclastic and siliciclastic sedimentary interbeds (Fig. 11). The full volcanic succession,
387 encountered in well 15/21-3, contains two repeated sequences of hyaloclastite to tabular lava
388 flows.

389 *Volcanic Facies Interpretation*

390 The presence of hyaloclastite indicates the area was at times subaqueous, with lava building
391 out into a standing water body. Thick tabular lava flows indicate large volumes of magma with
392 a fast effusion rate (Walker 1971), likely being erupted into an area of increased

393 accommodation space allowing inflation of individual flows. The volcanic wireline facies
394 interpreted in the northern Witch Ground Graben are typical of flood basalt eruptions
395 (Jerram *et al.* 2009; Nelson *et al.* 2009; Millet *et al.* 2016a). The repetition of subaqueous
396 hyaloclastite overlain by subaerial tabular lava flows in well 15/21-3 (Fig. 11) indicates that
397 relative water level rose during continued volcanic eruption, either by eustatic sea level rise
398 or active subsidence in the area.

399 *Northern Witch Ground Graben Summary*

400 No volcanic edifice nor associated magmatic plumbing system is visible on the available seismic
401 data in the northern Witch Ground Graben. We see no positive evidence on seismic to
402 support the interpretation of a large-scale central volcano in the Ivanhoe area (Block 15/23).
403 The volcanic sequence thins northwards from ~1.5 km thick in the centre of the RVP to ~0.4
404 km thick in the northern Witch Ground Graben (Fig. 1). The northwards thinning of the
405 volcanic sequence leads us to speculate that the extrusives of the Rattray Volcanics Member
406 in the northern Witch Ground Graben area were sourced from the Buchan-Glenn Fissure
407 System, ~37 km to the southeast in Blocks 21/04 and 21/05 (Fig. 8 inset map).

408 ***Fisher Bank Basin***

409 A large sub-circular positive magnetic anomaly of magnitude ~350 nT and diameter ~30 km
410 is present in the Fisher Bank Basin (Fig. 12a). This sub-circular shape is typical of igneous
411 centres elsewhere on the UKCS (Archer *et al.* 2005; Emeleus & Bell 2005; Schofield *et al.*
412 2017b). Smith & Ritchie (1993) interpreted the Fisher Bank Volcanic Centre to be almost
413 coincident with the peak of the magnetic anomaly. The volcanic centre was identified on
414 seismic data from the interpreted thickening of the volcanic sequence into the Fisher Bank
415 Basin, and a 'structural culmination' at the base of the Upper Jurassic (Smith & Ritchie 1993).

416 No wells penetrate to Jurassic level in the centre of the Fisher Bank Basin, though several
417 wells penetrate the Middle Jurassic towards the flanks of the basin (Fig. 12b). The Fisher Bank
418 Basin formed during Late Jurassic rifting, after the volcanism (Clark *et al.* 1993) and therefore
419 wells on the basin flanks should contain a similar Rattray sequence to the undrilled Rattray in
420 the depths of the basin.

421 *Volcanic Thickness and Facies around the Fisher Bank Basin*

422 The Rattray Volcanics Member is >800 m thick on the northern flanks of the Fisher Bank
423 Basin (16/29a-8) and thins southwards (624 m in 22/05b-4). The Middle Jurassic sequence
424 thickness is shown on seismic line F-F' (Fig. 12d/e), with seismic mapping indicating that it thins
425 southwards into the Fisher Bank Basin, contrary to the thickness map of Husmo *et al.* (2002)
426 (Fig. 12c). Investigation of the Rattray volcanic wireline facies on the flanks of the Fisher Bank
427 Basin indicates the volcanic sequence is dominated by compound basaltic lava flows and
428 volcanoclastic sedimentary rocks (e.g. 16/29a-8, 22/05b-4) (Fig. 12b), with the proportion of
429 sedimentary material in the volcanic sequence increasing southwards (Fig. 12b). The Middle
430 Jurassic succession in 22/05b-4 includes a thick (~100 m) Pentland Formation siliciclastic
431 sequence of sandstone, claystone and coal above the Rattray Volcanics Member. A similar
432 siliciclastic sequence is found overlying the volcanics in well 22/02-2 (~286 m), while well
433 22/07-1 on the Forties-Montrose High contains a 123 m thick Pentland Formation sandstone
434 and coal package but does not contain the Rattray Volcanics Member.

435 *Thickness and Facies Interpretation*

436 The overall southwards-decrease in thickness of the volcanic pile and the change in facies to
437 predominantly compound flows and sedimentary rocks indicates the Fisher Bank Basin was
438 distal to the volcanic source. The presence of thick Middle Jurassic siliciclastic sedimentary

439 rocks above the volcanics indicates the Fisher Bank area was a subsiding sedimentary
440 depocentre after volcanism in the area ceased, before the onset of Late Jurassic rifting. It is
441 therefore likely that the relatively thin Rattray succession in the south of the Fisher Bank Basin
442 is due to cessation of volcanism reaching the basin, rather than emplacement and subsequent
443 erosion.

444 *Seismic Line G-G': NW-SE across the Fisher Bank Basin*

445 The Middle Jurassic seismic package undulates and thins southwards across the Fisher Bank
446 Basin from ~630m (0.295 s) to ~270m (0.129 s) against the bounding fault to the Jaeren High
447 (Fig. 13(1)). Middle Jurassic strata appear to be domed upwards in the centre of the basin (Fig.
448 13(2)) and are onlapped by continuous seismic reflections of Late Jurassic age. A package with
449 limited internal reflectivity is present in the sub-Rattray sequence beneath this central
450 structure, but towards the basin margins a thick (~1.1 km, ~0.5 s TWT) package with faint
451 continuous reflections is present (Fig. 13(3)).

452 *Seismic Line G-G' Interpretation*

453 No large-scale vent structure is observed in the Fisher Bank Basin. The area of limited internal
454 reflectivity beneath the Middle Jurassic is interpreted as a diapir of Permian Zechstein Group
455 halite, surrounded by pods of Triassic sedimentary rocks (Fig. 13(3)). Above the interpreted
456 salt diapir an antiform structure is visible in the top Upper Jurassic reflection (Fig. 13(4)),
457 similar to the top Upper Jurassic structure above a drilled halite diapir at the north-western
458 edge of the Fisher Bank Basin (wells 16/27-1A and 16/28-1 (Fig. 13(5)); see inset map Fig. 12a).
459 Beneath the interpreted halite diapir seismic imaging becomes less clear. However no obvious
460 discordant seismic reflections indicative of plumbing system of a central volcano are visible on
461 the available seismic data (Fig. 13).

463 We find no positive evidence of a volcanic source area in the Fisher Bank Basin. We interpret
464 the base Upper Jurassic structure as the top of a salt diapir, caused by upwelling of Zechstein
465 Group evaporites (Fig. 13). The Fisher Bank Basin is at the northern extent of the Zechstein
466 Group evaporite sequence (Glennie *et al.* 2003). Thick evaporite packages, including halite and
467 anhydrite, are drilled on the surrounding Forties-Montrose and Jaeren Highs with Triassic
468 sediments deposited in pods in areas of salt withdrawal (Smith *et al.* 1993). The undulation
469 observed in the Rattray seismic sequence across the basin is likely due to movement of
470 Zechstein Group halite, which influences Jurassic sedimentation in the area (Clark *et al.* 1993).

471 The southwards-thinning Pentland Formation sequence and increasing proportion of
472 sedimentary material in the Fisher Bank Basin indicates the area was distal to the site of
473 volcanic eruption. The underlying cause of the positive magnetic anomaly in the Fisher Bank
474 Basin is therefore unclear and is discussed below. We suggest the extrusives of the Rattray
475 Volcanics Member in the Fisher Bank Basin and surrounding areas were likely sourced from
476 the Buchan-Glenn Fissure System, ~45 km to the northwest (Fig. 8 inset map).

477 **Discussion**

478 ***Eruption style of the Rattray Volcanic Province***

479 The identification of feeder dykes and small associated volcanic edifices in the centre of the
480 RVP indicates the volcanics were effused in a series of low-viscosity flood basalt eruptions
481 from at least one fissure system. The Buchan-Glenn Fissure System trends WSW-ENE across
482 the Buchan-Glenn Horst and, given its position in the centre of the RVP where the lava pile
483 is thickest, was likely the primary source area for the lavas. Magma conduits can be re-
484 exploited during later eruptions (Needham *et al.* 2011); it is possible that the area of the

485 Buchan-Glenn Fissure System was the site of several pulses of magmatism during the eruption
486 of the Rattray Volcanics Member.

487 In addition to the Buchan-Glenn Fissure System, there are likely many more fissure
488 vents associated with the RVP that remain as yet unidentified. Overprinting of earlier fissures
489 by other later lava flows may obscure fissure vents in seismic data. The identification of a
490 series of maar craters on the Renee Ridge by Stewart (1999) indicates that this area may also
491 have been the location of a volcanic fissure. However, as this area is outside the extent of our
492 available 3D seismic data we cannot investigate further. We suggest it is likely that other
493 volcanic fissures may be present across the Forties-Montrose High area, given the thickness
494 of the volcanic pile across that region (0.8-1.0 km). However, the presence of thick Zechstein
495 Group evaporites across the Forties-Montrose High creates uncertainty in interpreting
496 possible sub-vertical reflections associated with potential feeder dykes.

497 We do not see any large-scale volcanic vent structures in the available seismic data,
498 nor kilometre-scale suites of intrusive sill complexes or plutonic magma chambers in the
499 Rattray subsurface indicative of central complex plumbing systems. We find no evidence in
500 seismic data to support the interpretation of a series of large central volcanoes sourcing the
501 Rattray volcanism.

502 ***Influence of structural lineaments on volcanism***

503 While the main phase of rifting forming the trilete rift system in the Central North Sea
504 occurred during the Late Jurassic (Fraser *et al.* 2002), initiation of Jurassic rifting in the triple
505 junction area is thought to have begun during the Bathonian-Callovian in the Middle Jurassic
506 (Boldy & Brealey 1990; Davies *et al.* 1999; Stewart 1999; Husmo *et al.* 2002) and has previously
507 been suggested to exert a control on the distribution of the Rattray Volcanics (Howitt *et al.*
508 1975; Woodhall & Knox 1979). The initial phase of Jurassic rifting in the Bathonian-Callovian

509 was focussed along N-S Viking Graben trending faults and NE-SW Caledonian-trending faults
510 (Boldy & Brealey 1990; Erratt *et al.* 1999). The Caledonian-trending faults include the offshore
511 extension of the Highland Boundary Fault, which can be traced across the Central North Sea
512 from onshore Scotland to Norway (Doré & Gage 1987; Zanella *et al.* 2003). It strikes WSW-
513 ENE through the triple junction area and is approximately coincident with the Buchan-Glenn
514 Fissure System (Fig. 14), which trends in a similar orientation. The coincident positions of the
515 Buchan-Glenn Fissure System and the Highland Boundary Fault, and their shared WSW-ENE
516 orientation, suggests Caledonian structural lineaments may have influenced the opening of
517 Middle Jurassic volcanic fissure systems.

518 The pre-rift geometry of the Rattray Volcanics Member (Fig. 10) indicates the eruption
519 of the Rattray Volcanics Member occurred prior to the main phase of Late Jurassic rifting, as
520 suggested by Underhill & Partington (1993). However, it is possible that the initiation of
521 extension during the Middle Jurassic reactivated pre-existing Caledonide structural
522 weaknesses which were then exploited during volcanism. This link remains speculative;
523 quantitative analyses of the trends of the fissures and the Caledonian lineaments is needed to
524 investigate any relationship further.

525 ***Relationship of Rattray Volcanics Member to magnetic anomalies***

526 The Buchan-Glenn Fissure System is coincident with the WSW-ENE oriented elongate
527 magnetic anomaly of the Buchan-Glenn Horst, with the deep-rooted feeder dykes likely
528 associated with the positive magnetic response. The Fisher Bank magnetic anomaly (Fig. 14a)
529 displays a sub-circular shape analogous to the igneous centres seen along the west of Scotland
530 and offshore along the Northeast Atlantic Margin, but is not associated with a Middle Jurassic
531 volcano. The magnetic anomaly may alternatively represent a Jurassic intrusion associated
532 with Rattray magmatism without resulting in surface volcanism in the Fisher Bank Basin.

533 Woodhall & Knox (1979) suggest a large mafic intrusion is buried at depths of around 8 km
534 in the Fisher Bank Basin, although note its link to the Rattray volcanism is unknown. We
535 observe no evidence in seismic data linking the Fisher Bank magnetic anomaly to the RVP, and
536 explore an alternative explanation.

537 The Fisher Bank magnetic anomaly is of similar size and shape to other magnetic
538 anomalies on the UKCS (Fig. 14). Two similar sub-circular magnetic anomaly highs in the
539 Faroe-Shetland Basin (Fig. 14b) were originally interpreted as Palaeogene volcanic centres
540 associated with the formation of the North Atlantic Igneous Province, named the Westray
541 and Judd Central Complexes (Naylor *et al.* 1999). Later hydrocarbon drilling showed that this
542 interpretation was incorrect. The magnetic anomaly highs are caused by older (Westray dated
543 as late Precambrian, 204/15-2 end of well report) granite and granodiorite plutonic intrusions
544 unrelated to Palaeogene volcanism, now called the Westray and Cambo Highs (Watson *et al.*
545 2017). We suggest the Fisher Bank magnetic anomaly may represent a similar older intrusive
546 body with no relation to Rattray volcanism.

547 The subduction of Avalonia under Laurentia in the Caledonian Orogeny emplaced a
548 series of mafic and granitic plutons forming the Grampian Caledonides across NE Scotland
549 and Scandinavia on the Grampian terrane north of the Highland Boundary Fault (Stephenson
550 *et al.* 2000). The onshore magnetic anomaly map of Scotland displays circular magnetic
551 anomaly highs (e.g. the Cairngorm granite, Fig. 14c), of similar size (~30 km in diameter) to
552 the anomaly in the Fisher Bank Basin. Positive sub-circular magnetic anomalies offshore
553 northeast Scotland (Fig. 14d) are presumed to represent the continuation of the Grampian
554 Caledonide plutonic intrusions (Gatliff *et al.* 1994). Caledonian plutons are drilled in the Moray
555 Firth (Fig. 14e) and to the NE of the RVP in the Norwegian sector (Fig. 14f), with emplacement
556 ages dated as Middle Ordovician (463Ma in well Nor. 16/5-1) to Late Silurian (421Ma in Nor.
557 16/1-4) (Slagstad *et al.* 2011).

558 The Fisher Bank magnetic anomaly is south of the HBF on the Midland Valley Terrane.
559 Similar sized and shaped magnetic anomalies on the Midland Valley terrane to that of the
560 Fisher Bank Basin are also found across the West Central Shelf (Fig. 14g/h), between mainland
561 Scotland and the Central Graben (Fig. 1(a)). The basement rocks causing these magnetic
562 anomalies have not been drilled but are assumed to be deeply buried older igneous plutons
563 rather than associated with Middle Jurassic volcanism, due to their location away from the
564 RVP. We therefore suggest that given the presence of Caledonian plutons surrounding the
565 triple junction, and the lack of volcanic structures in the Fisher Bank Basin, the Fisher Bank
566 magnetic anomaly may be a similar Caledonian-aged intrusion, unrelated to the later Middle
567 Jurassic RVP.

568 *Ratray Magma Reservoir*

569 The position and depth of Ratray magma reservoir is unknown, as is its effect on geophysical
570 anomalies in the area. We have interpreted the Ratray Volcanics Member to be sourced from
571 a series of fissure eruptions from deep-rooted feeder dykes connected to a lower crustal
572 magma reservoir. We suggest the positive magnetic anomalies in the western area of the RVP
573 (e.g. Ivanhoe magnetic anomaly) do not represent upper crustal magma chambers associated
574 with central volcanoes, but may be associated with the deeply buried magma reservoir
575 sourcing the fissure eruptions. Magnetic and gravity modelling has been conducted on
576 geophysical anomalies across the UKCS (Donato & Tully 1981, 1982; Donato *et al.* 1983;
577 Archer *et al.* 2005); modelling of the anomalies at the triple junction may help elucidate the
578 depth, shape and composition of the Ratray magma reservoir.

579 ***Implications for Sub-Volcanic Hydrocarbon Prospectivity***

580 The lack of large-scale suites of igneous intrusions beneath the Rattray Volcanics Member in
581 the Witch Ground Graben, Buchan-Glenn Horst and Fisher Bank Basin areas has implications
582 for the extent of potential pre-Middle Jurassic hydrocarbon reservoirs and source rocks, with
583 the gross sedimentary rock volume beneath the extrusive volcanic cover likely greater than
584 previously supposed. Hydrocarbon accumulations in pre-Middle Jurassic reservoirs are found
585 across the triple junction area, e.g. Devonian sandstones (Edwards 1991; Gambaro & Currie
586 2003), Carboniferous sandstones and Permian Zechstein Group carbonates (Harker *et al.*
587 1991) and Triassic Skagerrak Formation sandstones (Samuel *et al.* 2005). The presence of pre-
588 Middle Jurassic hydrocarbon reservoirs around the triple junction indicates the possibility of
589 similar unexplored reservoir units beneath the RVP.

590 A schematic comparison of the likely sub-volcanic stratigraphy associated with the
591 previous volcanic centre eruption model and that of the revised fissure eruption model is
592 shown in Figure 15. The absence of a central volcano and associated plumbing system in the
593 undrilled Fisher Bank Basin (Fig. 15(a)) suggests thick pre-Middle Jurassic sedimentary units,
594 including potential Triassic sandstone reservoirs, may be present in the area. An extension of
595 the Triassic play, or older Permian, Carboniferous or Devonian plays, in the Fisher Bank Basin
596 may have been largely overlooked.

597 The Witch Ground Graben (Fig. 15(b)) and Buchan-Glenn Horst (Fig. 15(c)) contain
598 much thicker volcanic sequences than the Fisher Bank Basin. They too lack large igneous
599 intrusive complexes, suggesting that extensive sedimentary sequences are present beneath
600 the Rattray Volcanics Member. However, drilling for any pre-Middle Jurassic plays in these
601 areas would necessitate penetrating over a kilometre or more of volcanic material, which may
602 present a variety of drilling issues (Archer *et al.* 2005; Millett *et al.* 2016b).

603 The Rattray Volcanics Member overlies a thin Zechstein Group carbonate sequence
604 on top of the Devonian-Carboniferous Old Red Sandstone (ORS) Group on the Buchan-

605 Glenn Horst (Fig. 6). The ORS is the reservoir unit in the Buchan oilfield ~50 km west along
606 the Buchan-Glenn Horst structure. Although the Buchan field ORS is shallower (~3 km depth),
607 the possibility of oil-bearing ORS beneath the Rattray further east on the Buchan-Glenn Horst
608 (blocks 21/03, 21/04 and 21/05) cannot be ruled out. However, the presence of igneous dykes
609 in the Buchan-Glenn Horst area adds further complexity to the consideration of any pre-
610 volcanic hydrocarbon plays; any pre-Middle Jurassic plays beneath the Rattray Volcanics on
611 the Buchan-Glenn Horst may be compartmentalised by the feeder dyke swarm (Rateau *et al.*
612 2013).

613 Palaeozoic petroleum systems in the UKCS have recently become a subject of
614 renewed interest in the 21st Century Exploration Road Map (21CXR) Palaeozoic project
615 (Monaghan *et al.* 2015, 2016). We suggest the identification of the potential for a large
616 unexplored gross sedimentary rock volume immediately beneath the Rattray Volcanics
617 Member indicates that the Palaeozoic (and potential Triassic) petroleum system in the triple
618 junction area of the Central North Sea (Quads 15, 16, 21 and 22) warrants further study.

619 **Conclusions**

620 We have reviewed previous interpretations of mechanisms for the eruption of the Middle
621 Jurassic Rattray Volcanics Member at the triple junction of the North Sea rift system. With
622 the benefit of 3D seismic data we have shown there are likely no central volcanoes associated
623 with Rattray volcanism. The Rattray Volcanics were instead extruded in a series of fissure
624 eruptions from WSW-ENE trending fissure zones, including the Buchan-Glenn Fissure System.

625 The presence of thick sequences (up to ~70 m) of hyaloclastite as well as
626 phreatomagmatic vents and craters in the RVP indicates the volcanism occurred in a wetter
627 environment than previously thought.

628 The pre-existing NE-SW Caledonide trend has previously been shown to control the
629 orientation of faulting during the initiation of the North Sea rift; we suggest it is likely the
630 Caledonian trend controlled the emplacement of the Rattray Volcanics during the initial stages
631 of extension in the triple junction area during the Middle Jurassic.

632 The Fisher Bank Basin magnetic anomaly previously interpreted as a Middle Jurassic
633 volcanic centre may be linked to a deeply buried igneous pluton of Caledonian age.

634 The lack of large intrusive complexes beneath the Rattray Volcanics Member indicates
635 that pre-Middle Jurassic sedimentary sequences are likely more extensive than previously
636 thought. Pre-Middle Jurassic reservoir and source rock potential in the Rattray area may
637 therefore have been underestimated. However, the feeder dykes may cause
638 compartmentalisation of pre-volcanic reservoirs.

639 We have shown how the use of 3D seismic data and tools such as frequency
640 decomposition can help elucidate the presence of previously unidentified igneous dykes, which
641 has implications for basin development and possible effects on petroleum systems. This
642 workflow could aid interpretation in other basins where intrusive igneous activity is thought
643 to influence hydrocarbon migration pathways.

644 **Acknowledgements**

645 PGS are thanked for the generous donation of the MegaSurveyPlus and MegaSurvey 3D
646 seismic data sets. The British Geological Survey are thanked for the generous donation of
647 Digital Magnetic Anomaly data over the Central North Sea. Nexen are thanked for the use of
648 the AM852D1009 2D seismic data. Well and 2D seismic data were downloaded from the UK
649 Oil & Gas Common Data Access (CDA) portal. Offshore gravity and other magnetic anomaly
650 data were accessed on the BGS Offshore GeoIndex. GB onshore aeromagnetic data was
651 downloaded from the BGS Open Geoscience website. Interpretation was carried out using

652 IHS Kingdom, Foster Findlay Associates' (FFA) GeoTeric and Schlumberger Techlog software.
653 AQ thanks Jonathon Hardman for his advice on spectral decomposition and Niall Mark and
654 Jessica Pugsley for their helpful discussions. We would like to acknowledge John Dixon who
655 pioneered the work on the Triple Junction and who was a key mentor to both NS and JRU.
656 Craig Magee and an anonymous reviewer are thanked for their suggestions which substantially
657 improved this manuscript.

658 **Funding**

659 This work is part of AQ's PhD research which is funded by the Carnegie Trust for the
660 Universities of Scotland. AQ would like to thank the Carnegie Trust for their continued
661 support.

662 **References**

- 663 Archer, S.G., Bergman, S.C., Iliffe, J., Murphy, C.M. & Thornton, M. 2005. Palaeogene igneous
664 rocks reveal new insights into the geodynamic evolution and petroleum potential of the
665 Rockall Trough, NE Atlantic Margin. *Basin Research*, **17**, 171–201.
- 666 Bartetzko, A., Delius, H. & Pechinig, R. 2005. Effect of compositional and structural variations
667 on log responses of igneous and metamorphic rocks. I: mafic rocks Harvey, In: P. K.,
668 Brewer, T. S., Pezard, P. A. & Petrov, V. A. (eds). *Petrophysical Properties of Crystalline*
669 *Rocks*. Geological Society Special Publications., **240**, 255–278.
- 670 Bassett, M.G. 2003. Sub-Devonian geology. In: Evans, D., Graham, C., Armour, A. & Bathurst,
671 P. (eds) *The Millennium Atlas: Petroleum Geology of the Central and Northern North Sea*.
672 London, The Geological Society of London, 61-63.
- 673 Boldy, S.A.R. & Brealey, S. 1990. Timing, nature and sedimentary result of Jurassic tectonism
674 in the Outer Moray Firth. In: Hardman, R.F.P. & Brooks, J. (eds). *Tectonic Events*
675 *Responsible for Britain's Oil and Gas Reserves*, Geological Society Special Publications., **55**,
676 259–279.
- 677 Bruce, D.R.S. & Stemmerik, L. 2003. Carboniferous. In: Evans, D., Graham, C., Armour, A. &
678 Bathurst, P. (eds) *The Millennium Atlas: Petroleum Geology of the Central and Northern North*
679 *Sea*. London, The Geological Society of London, 83-89.
- 680 Cameron, T.D.J. 1993. 4. Triassic, Permian and pre-Permian of the Central and Northern
681 North Sea. In: Knox, R. W. O'B. & Cordey, W. G. (eds) *Lithostratigraphic Nomenclature*
682 *of the UK North Sea*. Nottingham, British Geological Survey.
- 683 Chalmers, J.A. & Western, P.G. 1979. A Tertiary igneous centre north of the Shetland Islands.
684 *Scottish Journal of Geology*. **15**(4). 333-341.
- 685 Clark, D.N., Riley, L.A. & Ainsworth, N.R. 1993. Stratigraphic, structural and depositional
686 history of the Jurassic in the Fisher Bank Basin , UK North Sea. In: Parker, J. R. (ed.)

- 687 *Petroleum Geology of Northwest Europe: Proceedings of the 4th Conference*. The Geological
688 Society, London, 415–424.
- 689 Cohen, K.M., Harper, D.A.T., Gibbard, P.L. & Fan, J.X. 2013. The ICS International
690 Chronostratigraphic Chart. *Episodes*, **36**, 199–204.
- 691 Copestake, P., Sims, A.P., Crittenden, S., Hamar, G.P., Ineson, J.R., Rose, P.T. & Tringham,
692 M.E. 2003. Lower Cretaceous. In: Evans, D., Graham, C., Armour, A. & Bathurst, P. (eds)
693 *The Millennium Atlas: Petroleum Geology of the Central and Northern North Sea*. London, The
694 Geological Society of London, 191–211.
- 695 Davies, R.J., O'Donnell, D., Bentham, P.N., Gibson, J.P.C., Curry, M.R., Dunay, R.E. & Maynard,
696 J.R. 1999. The origin and genesis of major Jurassic unconformities within the triple
697 junction area of the North Sea, UK. In: Fleet, A. J. & Boldy, S. A. R. (eds) *Petroleum Geology*
698 *of Northwest Europe: Proceedings of the 5th Conference*. The Geological Society, London,
699 117–131.
- 700 Deegan, C.E. & Scull, B.J. 1977. *A standard lithostratigraphic nomenclature for the Central and*
701 *Northern North Sea*. Institute of Geological Sciences Report 77/25; NPD-Bulletin No.1.
- 702 Dixon, J.E., Fitton, J.G. & Frost, R.T.C. 1981. The Tectonic Significance of Post-Carboniferous
703 Igneous Activity in the North Sea Basin. In: Illing, L. V. & Hobson, G. D. (eds): *Petroleum*
704 *Geology of the Continental Shelf of North-West Europe*. London, Institute of Petroleum, 121–
705 137.
- 706 Donato, J.A. & Tully, M.C. 1981. A Regional Interpretation of North Sea Gravity Data. In:
707 Illing, L. V. & Hobson, G. D. (eds): *Petroleum Geology of the Continental Shelf of North-West*
708 *Europe*. London, Institute of Petroleum, 65–75.
- 709 Donato, J.A. & Tully, M.C. 1982. A proposed granite batholith along the western flank of the
710 North Sea Viking Graben. *Geophysical Journal of the Royal Astronomical Society*, **69**, 187–
711 195.
- 712 Donato, J.A., Martindale, W. & Tully, M.C. 1983. Buried granites within the Mid North Sea
713 High. *Journal of the Geological Society*, **140**, 825–837.
- 714 Doré, A.G. & Gage, M.S. 1987. Crustal alignments and sedimentary domains in the evolution
715 of the North Sea, NE Atlantic Margin and Barents Shelf. In: Brooks, J. & Glennie, K. (eds)
716 *Petroleum Geology of North West Europe*. Graham & Trotman, 1131–1148.
- 717 Edwards, C.W. 1991. The Buchan Field, Blocks 20/5a, 21/1a, UK. North Sea. In: Abbots, I.L.
718 (ed). *United Kingdom Oil and Gas Fields, 25 years commemorative Volume*. Geological
719 Society, London, Memoirs, **14**, 253–260.
- 720 Emeleus, C.H. & Bell, B.R. 2005. *British Regional Geology: The Palaeogene Volcanic Districts of*
721 *Scotland (Fourth Edition)*. Nottingham, British Geological Survey.
- 722 Erratt, D., Thomas, G.M. & Wall, G.R.T. 1999. The evolution of the Central North Sea Rift.
723 In: Fleet, A.J. & Boldy, S.A.R. (eds). *Petroleum Geology of Northwest Europe: Proceedings of*
724 *the 5th Conference*, The Geological Society, London. 63–82.
- 725 Fall, H.G., Gibb, F.G.F. & Kanaris-Sotiriou, R. 1982. Jurassic volcanic rocks of the northern
726 North Sea. *Journal of the Geological Society of London*, **139**, 277–292.
- 727 Fraser, S.I., Robinson, A.M., Johnson, H.D., Underhill, J.R., Kadolsky, D.G.A., Connell, R.,
728 Johannessen, P. and Ravnås, R. 2002. Upper Jurassic. In: Evans, D., Graham, C., Armour,
729 A. & Bathurst, P. (eds) *The Millennium Atlas: Petroleum Geology of the Central and Northern*
730 *North Sea*. London, The Geological Society of London, 157–189.
- 731 Gambaro, M. & Currie, M. 2003. The Balmoral, Glamis and Stirling Fields, Block 16/21, UK
732 Central North Sea. In: Gluyas, J. G. & Hitchens, H. M. (eds) *United Kingdom Oil and Gas*
733 *Fields, Commemoration Millennium Volume*. London, Geological Society, 395–413.
- 734 Gatliff, R.W., Richards, P.C., Smith, K., Graham, C.C., McCormac, M., Smith, N.J.P., Long, D.,
735 Cameron, T.D.J., Evans, D., Stevenson, A.G., Bulat, J. & Ritchie, J.D. 1994. *United Kingdom*
736 *Offshore Regional Report: The Geology of the Central North Sea*. London, British Geological

- 737 Survey.
- 738 Gibb, F.G.F. & Kanaris-Sotiriou, R. 1976. Jurassic igneous rocks of the Forties Field. *Nature*,
739 **260**, 23–25.
- 740 Glennie, K.W., Higham, J. & Stemmerik, L. 2003. Permian. In: Evans, D., Graham, C., Armour,
741 A. & Bathurst, P. (eds) *The Millennium Atlas: Petroleum Geology of the Central and Northern*
742 *North Sea*. London, The Geological Society of London, 91–103.
- 743 Goldsmith, P.J., Hudson, G. & Van Veen, P. 2003. Triassic. In: Evans, D., Graham, C., Armour,
744 A. & Bathurst, P. (eds) *The Millennium Atlas: Petroleum Geology of the Central and Northern*
745 *North Sea*. London, The Geological Society of London, 105–127.
- 746 Gradstein, F.M., Ogg, J.G., Schmitz, M. & Ogg, G. 2012. *The Geologic Time Scale 2012*. Elsevier
747 B.V.
- 748 Gudmundsson, A. 1987. Formation and mechanics of magma reservoirs in Iceland. *Geophysical*
749 *Journal of the Royal Astronomical Society*, **91**, 27–41.
- 750 Hardman, J., Schofield, N., Jolley, D., Hartley, A., Holford, S. & Watson, D. 2018. Controls on
751 the distribution of volcanism and intra-basaltic sediments in the Cambo–Rosebank
752 region, West of Shetland. *Petroleum Geoscience*, petgeo2017-061.
- 753 Harker, S.D., Green, S.C.H. & Romani, R.S. 1991. The Claymore Field, Block 14/19, UK North
754 Sea. In: Abbotts, I. L. (ed.) *United Kingdom Oil and Gas Fields 25 Years Commemorative*
755 *Volume*. Geological Society, 269–278.
- 756 Heiken, G.H. 1971. Tuff rings: Examples from the Fort Rock-Christmas Lake Valley Basin,
757 south-central Oregon. *Journal of Geophysical Research*, **76**, 5615–5626.
- 758 Holford, S.P., Schofield, N. & Reynolds, P. 2017. Subsurface fluid flow focused by buried
759 volcanoes in sedimentary basins: Evidence from 3D seismic data, Bass Basin, offshore
760 southeastern Australia. *Interpretation*, **5**, SK39-SK50.
- 761 Howitt, F., Aston, E.R. & Jacqué, M. 1975. The Occurrence of Jurassic Volcanics in the North
762 Sea. In: Woodland, A.W. (ed) *Petroleum and the Continental Shelf of Northwest Europe*,
763 Applied Science, Barking. 379–387.
- 764 Husmo, T., Hamar, G.P., Hoiland, O., Johannessen, E.P., Romuld, A., Spencer, A.M. &
765 Titterton, R. 2002. Lower and Middle Jurassic. In: Evans, D., Graham, C., Armour, A. &
766 Bathurst, P. (eds) *The Millennium Atlas: Petroleum Geology of the Central and Northern North*
767 *Sea*. London, The Geological Society of London, 129–155.
- 768 Jerram, D.A., Single, R.T., Hobbs, R.W. & Nelson, C.E. 2009. Understanding the offshore flood
769 basalt sequence using onshore volcanic facies analogues: an example from the Faroe-
770 Shetland basin. *Geological Magazine*. **146**(3), 353–367.
- 771 Johnson, H. & Lott, G.K. 1993. 2. Cretaceous of the Central and Northern North Sea. In:
772 Knox, R. W. O'B. & Cordey, W. G. (eds) *Lithostratigraphic Nomenclature of the UK North*
773 *Sea*. Nottingham, British Geological Survey.
- 774 Johnson, H.A.B., Leslie, A.B., Wilson, C.K., Andrews, I.J. & Cooper, R.M. 2005. *Middle Jurassic,*
775 *Upper Jurassic and Lower Cretaceous of the UK Central and Northern North Sea*. British
776 Geological Survey Research Report, RR/03/001, 42pp.
- 777 Jolley, D.W. & Bell, B.R. 2002. Genesis and age of the Erlend Volcano, NE Atlantic Margin. In:
778 Jolley, D.W. & Bell, B.R. (eds) *The North Atlantic Igneous Province: Stratigraphy, Tectonic,*
779 *Volcanic and Magmatic Processes*. Geological Society, London, Special Publications, **197**,
780 95–109. The Geological Society of London.
- 781 Jones, J.G. & Nelson P.H.H. The flow of basalt lava from air into water – its structural and
782 stratigraphic significance. *Geological Magazine*. **107**, 13–19.
- 783 Kallweit, R.S. & Wood L.C. 1982. The limits of resolution of zero-phase wavelets. *Geophysics*.
784 **47**, 1035–1046.
- 785 Kereszturi, G. & Németh, K. 2012. Monogenetic Basaltic Volcanoes: Genetic Classification,
786 Growth, Geomorphology and Degradation. In: Németh, K. (ed.) *Updates in Volcanology -*

- 787 *New Advances in Understanding Volcanic Systems*. InTech, 1–89.
- 788 Latin, D. & Waters, F.G. 1991. Melt generation during rifting in the North Sea. *Nature*, **351**,
789 559–562.
- 790 Latin, D. & Waters, F.G. 1992. Basaltic magmatism in the North Sea and its relationship to
791 lithospheric extension. *Tectonophysics*, **208**, 77–90.
- 792 Latin, D.M., Dixon, J.E. & Fitton, J.G. 1990a. Rift-related magmatism in the North Sea Basin.
793 In: Blundell, D. J. & Gibbs, A. D. (eds) *Tectonic Evolution of the North Sea Rifts*. Oxford,
794 Oxford Science Publications, 101–144.
- 795 Latin, D.M., Dixon, J.E., White, N.J. & Fitton, J.G. 1990b. Mesozoic magmatic activity in the
796 North Sea Basin: implications for stretching history. In: Hardman, R.F.P. & Brooks, J.
797 (eds). *Tectonic Events Responsible for Britain's Oil and Gas Reserves*, Geological Society,
798 London, Special Publications, **55**, 207–227.
- 799 Magee, C., Jackson, C.A.-L. & Schofield, N. 2014. Diachronous sub-volcanic intrusion along
800 deep water margins: insights from the Irish Rockall Basin. *Basin Research*. **26**, 85-105.
- 801 Marshall, J.E.A. & Hewett, A.J. 2003. Devonian. In: Evans, D., Graham, C., Armour, A. &
802 Bathurst, P. (eds) *The Millennium Atlas: Petroleum Geology of the Central and Northern North*
803 *Sea*. London, The Geological Society of London, 65-81.
- 804 McLean, C.E., Schofield, N., Brown, D.J., Jolley, D.W. & Reid, A. 2017. 3D seismic imaging of
805 the shallow plumbing system beneath the Ben Nevis Monogenetic Volcanic Field: Faroe-
806 Shetland Basin. *Journal of the Geological Society*. **174**, 468-485.
- 807 Millett, J.M., Hole, M.J., Jolley, D.W., Schofield, N. & Campbell, E. 2016a. Frontier exploration
808 and the North Atlantic Igneous Province: new insights from a 2.6 km offshore volcanic
809 sequence in the NE Faroe–Shetland Basin. *Journal of the Geological Society*, **173**, 320–336.
- 810 Millett, J.M., Wilkins, A.D., Campbell, E., Hole, M.J., Taylor, R.A., Healy, D., Jerram, D.A., Jolley,
811 D.W., Planke, A., Archer, S.G. & Blischke, A. 2016b. The geology of offshore drilling
812 through basalt sequences: Understanding operational complications to improve
813 efficiency. *Marine and Petroleum Geology*, **77**, 1177–1192.
- 814 Monaghan, A., Arsenikos, S., Callaghan, E., Ellen, R., Gent, C., Hannis, S., Henderson, A., Leslie,
815 G., Johnson, K., Kassyk, M., Kearsy, T., Kim, A., Kimbell, G., Quinn, M., Mclean, W.,
816 Millward, D., Pharaoh, T., Sankey, M., Smith, N., Ugana, C., Vane, C., Vincent, C. &
817 Williamson, P. 2015. *Palaeozoic Petroleum Systems of the Central North Sea/ Mid North Sea*
818 *High*. British Geological Survey Commissioned Report, CR/15/124, 105pp.
- 819 Monaghan, A., Johnson, K., Arsenikos, S., Callaghan, E., Fellgett, M., Hannis, S., Henderson, A.,
820 Leslie, G., Kearsy, T., Kim, A., Kimbell, G., Quinn, M., Mclean, W., Millward, D., Sankey,
821 M., Smith, N., Ugana, C., Vane, C., Vincent, C. & Williamson, P. 2016. *Palaeozoic Petroleum*
822 *Systems of the Orcadian Basin to Forth Approaches, Quadrants 6-21, UK*. In: British Geological
823 Survey Commissioned Report, CR/16/038. 67pp.
- 824 Naylor, P.H., Bell, B.R., Jolley, D.W., Durnall, P. & Fredsted, R. 1999. Palaeogene magmatism
825 in the Faeroe-Shetland Basin: influences on uplift history and sedimentation. In: Fleet, A.J.
826 & Boldy, S.A.R. (eds). *Petroleum Geology of Northwest Europe: Proceedings of the 5th*
827 *Conference*, London, 545–558.
- 828 Needham, A.J., Lindsay, J.M., Smith, I.E.M., Augustinus, P. & Shane, P.A. 2011. Sequential
829 eruption of alkaline and sub-alkaline magmas from a small monogenetic volcano in the
830 Auckland Volcanic Field, New Zealand. *Journal of Volcanology and Geothermal Research*.
831 **201**, 126-142.
- 832 Nelson, C.E., Jerram, D.A. & Hobbs, R.W. 2009. Flood basalt facies from borehole data:
833 implications for prospectivity and volcanology in volcanic rifted margins. *Petroleum*
834 *Geoscience*, **15**, 313–324.
- 835 Phillips, T.B., Magee, C., Jackson, C.A.L. & Bell, R.E. 2017. Determining the three-dimensional
836 geometry of a dike swarm and its impact on later rift geometry using seismic reflection

837 data. *Geology*, **46**, 119–122.

838 Planke, S. 1994. Geophysical response of flood basalts from analysis of wire line logs: Ocean
839 Drilling Program Site 642. Vøring volcanic margin. *Journal of Geophysical Research*, **99**(B5),
840 9279-9296.

841 Planke, S., Rasmussen, T., Rey, S. & Myklebust, R. 2005. Seismic characteristics and distribution
842 of volcanic intrusions and hydrothermal vent complexes in the Vøring and Møre basins.
843 In: Doré, A.G. & Vining, B.A. (eds). *Petroleum Geology: Northwest-Europe and Global
844 Perspectives – Proceedings of the 6th Petroleum Geology Conference*. London, The Geological
845 Society, 833-844.

846 Rateau, R., Schofield, N. & Smith, M. 2013. The potential role of igneous intrusions on
847 hydrocarbon migration, West of Shetland. *Petroleum Geoscience*, **19**, 259-272.

848 Reynolds, P., Brown, R.J., Thordarson, T. & Llewellyn, E.W. 2016. The architecture and shallow
849 conduits of Laki-type pyroclastic cones: insights into a basaltic fissure eruption. *Bulletin of
850 Volcanology*, **78**(5) 36.

851 Reynolds, P., Schofield, N., Brown, R.J. & Holford, S.P. 2018. The architecture of submarine
852 monogenetic volcanoes – insights from 3D seismic data. *Basin Research*, **30**, 437-451.

853 Richards, P.C., Lott, G.K., Johnson, H., Knox, R.W.O'B. & Riding, J.B. 1993. 3. Jurassic of the
854 Central and Northern North Sea. In: Knox, R. W. O'B. & Cordey, W. G. (eds)
855 *Lithostratigraphic Nomenclature of the UK North Sea*. Nottingham, British Geological Survey.

856 Ritchie, J.D., Swallow, J.L., Mitchell, J.G. & Morton, A.C. 1988. Jurassic ages from intrusives
857 and extrusives within the Forties Igneous Province. *Scottish Journal of Geology*, **24**, 81–88.

858 Samuel, A., Taylor, C., Richards, S., Warburton, I. & Highton, P. 2005. Armada Phase II and
859 Seymour Phase I. In: Doré, A. G. & Vining, B. A. (eds) *Petroleum Geology: Northwest Europe
860 and Global Perspectives - Proceedings of the 6th Petroleum Geology Conference*. London,
861 Geological Society, 675–686.

862 Schofield, N. & Jolley, D.W. 2013. Development of intra-basaltic lava-field drainage systems
863 within the Faroe-Shetland Basin. *Petroleum Geoscience*, **19**, 273–288.

864 Schofield, N., Holford, S.P. Millett, J., Brown, D.J., Jolley, D.W., Passey, S.R., Muirhead, D.,
865 Grove, C., Magee, C., Murray, J., Hole, M., Jackson, C.A.-L. & Stevenson, C. 2017a.
866 Regional magma plumbing and emplacement mechanisms of the Faroe-Shetland Sill
867 Complex: implications for magma transport and petroleum systems within sedimentary
868 basins. *Basin Research*. **29**, 41-63.

869 Schofield, N., Jolley, D., Holford, S., Archer, S., Watson, D., Hartley, A., Howell, J., Muirhead,
870 D., Underhill, J. & Green, P. 2017b. Challenges of future exploration within the UK
871 Rockall Basin. In: Bowman, M. & Levell, B. (eds) *Petroleum Geology of NW Europe: 50 Years
872 of Learning - Proceedings of the 8th Conference*, Geological Society, London, PGC8.37.

873 Slagstad, T., Davidsen, B. & Daly, J.S. 2011. Age and composition of crystalline basement rocks
874 on the Norwegian continental margin: offshore extension and continuity of the
875 Caledonian-Appalachian orogenic belt. *Journal of the Geological Society*, **168**, 1167–1185.

876 Smith, K. & Ritchie, J.D. 1993. Jurassic volcanic centres in the Central North Sea. In: Parker,
877 J.R. (ed.) *Petroleum Geology of Northwest Europe: Proceedings of the 4th Conference*. London,
878 The Geological Society, 519–531.

879 Smith, R.I., Hodgson, N. & Fulton, M. 1993. Salt control on Triassic reservoir distribution,
880 UKCS Central North Sea. In: Parker, J.R. (ed). *Petroleum Geology of Northwest Europe:
881 Proceedings of the 4th Conference*. The Geological Society, London, 547–557.

882 Stephenson, D., Bevins, R.E., Millward, D., Stone, P., Parsons, I., Highton, A.J. & Wadsworth,
883 W.J. 2000. *Caledonian Igneous Rocks of Great Britain*, Geological Conservation Review
884 Series No. 17, Joint Nature Conservation Committee. Peterborough. 648pp.

885 Stewart, S.A. 1999. Mid-Jurassic volcanic structures in the Outer Moray Firth Basin, UK.
886 *Journal of the Geological Society*, **156**, 487–499.

- 887 Surlyk, F., Dons, T., Clausen, C.K. & Higham, J. 2003. Upper Cretaceous. In: Evans, D.,
 888 Graham, C., Armour, A. & Bathurst, P. (eds) *The Millennium Atlas: Petroleum Geology of the*
 889 *Central and Northern North Sea*. London, The Geological Society of London, 213-233.
- 890 Thordarson, T. & Larsen, G. 2007. Volcanism in Iceland in historical time: Volcano types,
 891 eruption styles and eruptive history. *Journal of Geodynamics*, **43**, 118–152.
- 892 Thordarson, T. & Self, S. 1993. The Laki (Skaftár Fires) and Grímsvötn eruptions in 1973-
 893 1785. *Bulletin of Volcanology*, **55**, 233–263.
- 894 Underhill, J.R. 1998. Jurassic. In: Glennie, K. W. (ed.) *Petroleum Geology of the North Sea: Basic*
 895 *Concepts and Recent Advances*. Blackwell Science, 245–293.
- 896 Underhill, J.R. 2009. Role of intrusion-induced salt mobility in controlling the formation of the
 897 enigmatic ‘Silverpit Crater’, UK Southern North Sea. *Petroleum Geoscience*, **15**, 197–216.
- 898 Underhill, J.R. & Partington, M.A. 1993. Jurassic thermal doming and deflation in the North
 899 Sea: implications of the sequence stratigraphic evidence. In: Parker, J. R. (ed.) *Petroleum*
 900 *Geology of Northwest Europe: Proceedings of the 4th Conference*. London, The Geological
 901 Society, 337–345.
- 902 Walker, G.P.L. 1971. Compound and simple lava flows and flood basalts. *Bulletin Volcanologique*,
 903 **35**, 579–590.
- 904 Walker, G.P.L. 1995. Flood basalts versus central volcanoes and the British Tertiary Volcanic
 905 Province. In: Le Bas, M.J. (ed) *Milestones in Geology*, Geological Society of London Memoir,
 906 **16**, 195–202.
- 907 Walker, G.P.L. 2000. Basaltic Volcanoes and Volcanic Systems. In: Sigurdsson, H., Houghton,
 908 B., Rymer, H., Stix, J. & McNutt, S. (eds) *Encyclopedia of Volcanoes*. Academic Press, 283–
 909 289.
- 910 Wall, M., Cartwright, J., Davies, R. & McGrandle, A. 2010. 3D seismic imaging of a Tertiary
 911 Dyke Swarm in the Southern North Sea, UK. *Basin Research*, **22**(2), 181-194.
- 912 Watson, D., Schofield, N., Jolley, D., Archer, S., Finlay, A.J., Mark, N., Hardman, J. & Watton,
 913 T. 2017. Stratigraphic overview of Palaeogene tuffs in the Faroe – Shetland Basin, NE
 914 Atlantic Margin. *Journal of the Geological Society*, **174**, 627–645.
- 915 Watton, T.J., Wright, K.A., Jerram, D.A. & Brown, R.J. 2014. The petrophysical and
 916 petrographical properties of hyaloclastite deposits: Implications for petroleum
 917 exploration. *AAPG Bulletin*, **98**, 449–463.
- 918 Woodhall, D. & Knox, R.W.O’B. 1979. Mesozoic volcanism in the northern North Sea and
 919 adjacent areas. *Bulletin of the Geological Survey of Great Britain*, **70**, 34–56.
- 920 Wright, K.A., Davies, R.J., Jerram, D.A., Morris, J. & Fletcher, R. 2012. Application of seismic
 921 and sequence stratigraphic concepts to a lava-fed delta system in the Faroe-Shetland
 922 Basin, UK and Faroes. *Basin Research*, **24**, 91–106.
- 923 Zanella, E., Coward, M.P. & Mcgrandle, A. 2003. Crustal Structure. In: Evans, D., Graham, C.,
 924 Armour, A. & Bathurst.P. (eds) *The Millennium Atlas: Petroleum Geology of the Central and*
 925 *Northern North Sea*. London, The Geological Society of London, 35–43.

926
 927 **Fig. 1. A:** Map of the North Sea rift system with the position of the Rattray Volcanic Province
 928 at the triple junction of the Viking Graben, Central Graben and Outer Moray Firth Basin.
 929 Adapted from Fraser *et al.* 2002. **B:** Present-day thickness and structure map of the Rattray
 930 Volcanics Member constructed using well and seismic mapping. Structures adapted from
 931 Fraser *et al.* 2002. Volcanic centres of Smith & Ritchie (1993): I – Ivanhoe Volcanic Centre, G
 932 – Glenn Volcanic Centre, F – Fisher Bank Volcanic Centre.

933 **Fig. 2.** Stratigraphic column for the triple junction area of the Central North Sea. The Rattray
 934 Volcanics Member comprises part of the Middle Jurassic Pentland Formation in the Fladen
 935 Group, as does the Ron Volcanics Member in the West Central Graben. The Middle Jurassic

936 rocks sit unconformably on Triassic or older strata, with the majority of the Lower Jurassic
937 and uppermost Triassic having been eroded in the regional doming event creating the Intra-
938 Aalenian Unconformity. The Middle Jurassic strata are overlain by marine sedimentary rocks
939 of the Upper Jurassic. *Chart based on: Cohen et al. 2013. Stratigraphy based on: Palaeozoic:*
940 *Bassett 2003; Marshall & Hewett 2003; Bruce & Stemmerik 2003; Glennie et al. 2003;*
941 *Cameron 1993. Mesozoic: Cameron 1993; Richards et al. 1993; Johnson & Lott 1993;*
942 *Goldsmith et al. 2003; Fraser et al. 2002; Copestake et al. 2003; Surlyk et al. 2003.*

943 **Fig. 3. A:** Map of seismic surveys and well penetrations utilised in this study. Outline of
944 Rattray Volcanic Province in red. Positions of seismic lines included in this paper in yellow. **B:**
945 Polarity of 3D and 2D seismic data. A downwards increase in acoustic impedance is
946 represented by a negative amplitude response (trough), here displayed in blue.

947 **Fig. 4.** Frankenstein well log showing typical petrophysical characteristics of the main basaltic
948 volcanic facies in the Rattray Volcanic Province. The log is composed of examples from
949 different wells drilled through the Rattray Volcanics Member (wells highlighted on right hand
950 side). GR – Gamma ray log. Res – Deep resistivity log. Dens – Density log. Neut – Neutron
951 porosity log. DT – Acoustic travel time log.

952 **Fig. 5.** Depth to present-day Top Pentland Fm (s TWT) across the MS and MSP. Well
953 penetration depths to the Rattray Volcanics Mbr are highlighted. The Pentland Fm is
954 shallowest on structural highs such as the Piper Shelf (PS), Renee Ridge (RR) and Buchan-
955 Glenn Horst (BGH) (2.3-2.8 km depth) and deepest in Witch Ground Graben (WGG) and
956 Fisher Bank Basin (FBB) (>5 km depth). HH: Halibut Horst; FGS: Fladen Ground Spur; SVG:
957 South Viking Graben; NBG: North Buchan Graben; SBG: South Buchan Graben; FMH: Forties
958 Montrose High; JH: Jaeren High.

959 **Fig. 6. A:** Magnetic anomaly map of the Rattray area with the magnetic anomaly coincident
960 with the Buchan-Glenn Horst structure highlighted. Volcanic centres of Smith & Ritchie (1993)
961 indicated. I – Ivanhoe Volcanic Centre; G – Glenn Volcanic Centre; F – Fisher Bank Volcanic
962 Centre. Reproduced from the British Geological Survey Map data at the original scale of
963 1:50,000. Licence 2016/103 ED British Geological Survey. ©NERC. All rights reserved.
964 Positions of seismic lines shown in Figures 6, 7 and 9 are highlighted in the inset map. **B and**
965 **C (interpreted):** Seismic line A-A' W-E across the Buchan-Glenn Horst over the peak of
966 the magnetic anomaly. The Rattray Volcanics Member is ~1.2 km thick across this section of
967 the Buchan-Glenn Horst. It lies above a thin Permian carbonate succession above the
968 Devonian-Carboniferous Old Red Sandstone Group with laterally continuous seismic
969 reflections. There is no obvious large-scale volcanic vent structure observed in the Rattray
970 succession, nor kilometre-scale discordant seismic reflections in the sub-Rattray stratigraphy
971 which would indicate an intrusive sill complex feeding a large central volcano. A sill cross-cuts
972 the volcanic reflections in the Rattray package, indicative of later-stage intrusion which did
973 not feed the majority of the Rattray volcanism. Inclined seismic reflections in the Rattray
974 sequence downlap the substrate, likely a hyaloclastite delta.

975 **Fig. 7. A and B (interpreted):** Seismic line B-B' from N-S across Buchan-Glenn Horst
976 showing sub-vertical discontinuities through the Rattray and older strata. The discontinuities
977 in the centre of the horst do not show displacement of the volcanic seismic reflections and
978 are interpreted as igneous dykes rather than fault planes. The dykes intrude through the sub-
979 Rattray stratigraphy and the volcanics themselves, but are not found above the Rattray
980 Volcanics Member. The dykes would have been almost vertical when emplaced – the tilting is
981 due to rotation during later tectonic events.

982 **Fig. 8. A:** Spectral decomposition of flattened Top Rattray surface in the Buchan-Glenn Horst
983 area. **B:** Interpreted. Linear discontinuity of dykes in Fig. 7 is interpreted as a volcanic fissure
984 (1) sourcing lava flows. The linear fissure is a notably different morphology to the curvilinear
985 fault planes (2) formed after cessation of volcanism during Late Jurassic rifting. Five small
986 volcanic edifices are interpreted along the fissure (5), likely spatter or cinder cones formed
987 during fissure eruptions. **C:** Satellite image of Laki Fissure in Iceland, showing cones aligned
988 along fissure. **D:** Photograph of the Laki Fissure and cone-row courtesy of *Encyclopaedia*
989 *Britannica Online*.

990 **Fig. 9.** Seismic lines C-C' and D-D' SW-NE across the main fissure zone on the Buchan-Glenn
991 Horst and Renee Ridge intersection. Small volcanic edifices protrude from the Top Rattray
992 surface overlying chaotic reflections of the fissure zone. The vents are of different
993 morphologies: C-C' has the aspect ratio of a cinder cone (Heiken 1971) and D-D' of a tuff
994 cone (Heiken 1971) although the deep funnel-like shape in D-D' is also reminiscent of a maar-
995 diatreme, which have been previously identified in the RVP further west along Renee Ridge
996 (Stewart 1999). The presence of tuff cones/maars and hyaloclastite indicates that the eruption
997 of the Rattray Volcanics Member involved a high proportion of interaction with both surface
998 water and groundwater.

999 **Fig. 10. A:** Large positive magnetic anomaly in the northern Witch Ground Graben. Inset
1000 map shows position of seismic line in Fig. 10B and C. **B and C (interpreted):** Composite
1001 seismic line E-E' across peak of the magnetic anomaly. The Rattray Volcanics Member is
1002 downthrown to the north during Late Jurassic faulting. The volcanics package thins
1003 northwards from ~800 m beside the fault to ~419 m in well 15/23-1Z. It overlies a Permian
1004 sequence drilled in 15/23-1Z, the base of which is uncertain but is tentatively identified on a
1005 dim continuous 'soft' reflection. No volcanic vent structures are present in the Rattray
1006 succession, nor large scale discordant seismic reflections typical of an intrusive sill complex is
1007 visible in the Rattray subsurface in the Northern Witch Ground Graben. There does not
1008 appear to be any positive evidence on seismic to support the interpretation of a central
1009 volcano.

1010 **Fig. 11.** Volcanic facies in wells in the northern Witch Ground Graben area (well positions
1011 in Fig. 10 inset map). Thick tabular lava flows (1) indicate a high rate of effusion and ponding
1012 in areas of increased accommodation space. Hyaloclastite packages (2) are indicative of
1013 eruption of lava into a standing water body. The repetition of hyaloclastite capped by subaerial
1014 tabular lava flows in well 15/21-3 is indicative of relative base level rise, either by eustatic sea
1015 level rise or relative rise due to active subsidence in the basin. These facies are typical of flood
1016 basalt eruptions from fissure systems.

1017 **Fig. 12. A:** Fisher Bank Basin magnetic anomaly. Inset map shows positions of wells and
1018 seismic lines in Figures 12 and 13. **D and E (interpreted):** The Pentland Fm is interpreted
1019 on seismic data in this study to thin southwards into the Fisher Bank Basin, contrary to the
1020 thickness interpretation of Husmo *et al.* (2002) **(C).** **B:** Proportion of facies in Pentland Fm
1021 of wells surrounding Fisher Bank Basin on Middle Jurassic thickness map. The proportion of
1022 crystalline material (lavas and hyaloclastite) decreases towards the south of the Fisher Bank
1023 Basin while the proportion of volcanoclastic and siliciclastic sedimentary rocks increase. This
1024 facies change is likely to occur as the system becomes more distal to the source of the volcanic
1025 eruption.

1026 **Fig. 13.** Seismic line G-G' from NW to SE through Fisher Bank Basin over the peak of the
1027 magnetic anomaly. A ~0.5 s (~1.1 km) thick Permo-Triassic succession makes up the majority

I028 of the basin fill beneath the thin Middle Jurassic sequence. No obvious volcanic vent structure
I029 nor sub-volcanic intrusive complex is visible. The seismic culmination at base Upper Jurassic
I030 level is interpreted here as a diapir of Zechstein halite, drilled nearby in I6/28-I and I6/27-
I031 IA.

I032 **Fig. I4.** Magnetic anomaly map of UK Central North Sea, West of Shetland area and onshore
I033 Scotland courtesy of BGS. Positions of wells which have drilled Caledonian intrusions in the
I034 basement of CNS are shown **(e,f)**, surrounding the RVP. Fisher Bank magnetic anomaly is
I035 highlighted **(a)** along with similar shaped anomalies from across the UK and UKCS
I036 **(b,c,d,g,h)**. The majority of these magnetic anomalies are granitic intrusions emplaced during
I037 or prior to the Caledonian Orogeny, e.g. the Westray and Cambo Highs in the Faroe-Shetland
I038 Basin **(b)** and the onshore Grampian Caledonides **(c)**. Also highlighted is the Highland
I039 Boundary Fault, which intersects with the Rattray Volcanics Member around the Buchan-
I040 Glenn Fissure System in the same orientation (WSW-ENE).

I041 **Fig. I5.** Schematic cross sections across the RVP from the Piper Shelf in NW to the Jaeren
I042 High in SE (approximate position of cross-section on Fig. I) showing possible sub-volcanic
I043 stratigraphy implied by the volcanic centres model (above) and fissure system model (below).
I044 Fissure-fed volcanism from the Buchan-Glenn Fissure System and a lack of central volcanoes
I045 in the Witch Ground Graben and Fisher Bank Basins indicates a large un-intruded sedimentary
I046 gross rock volume is present beneath the RVP. Approximate positions of the seismic lines
I047 shown in figures 7, I0 and I3 are highlighted.

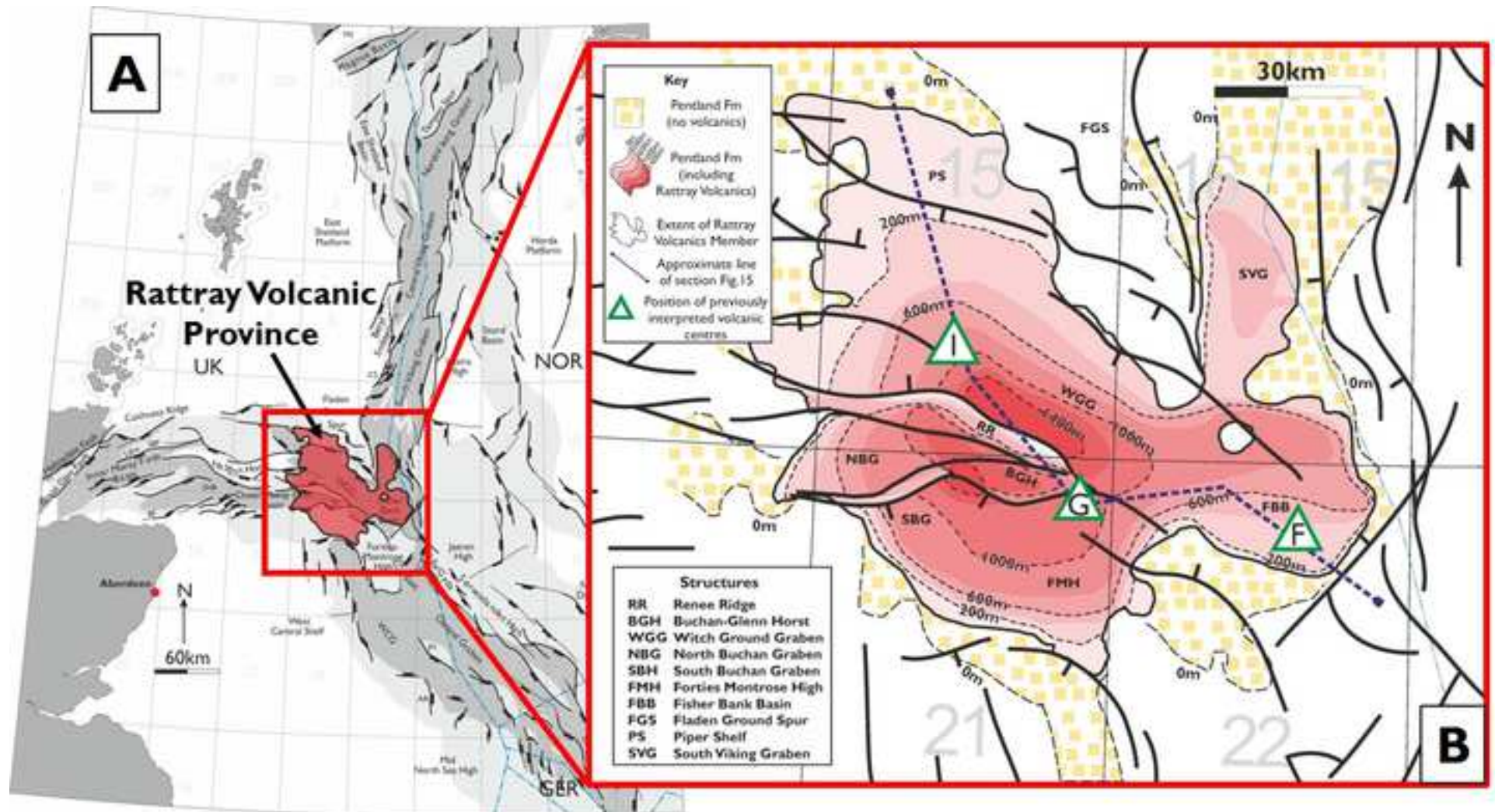
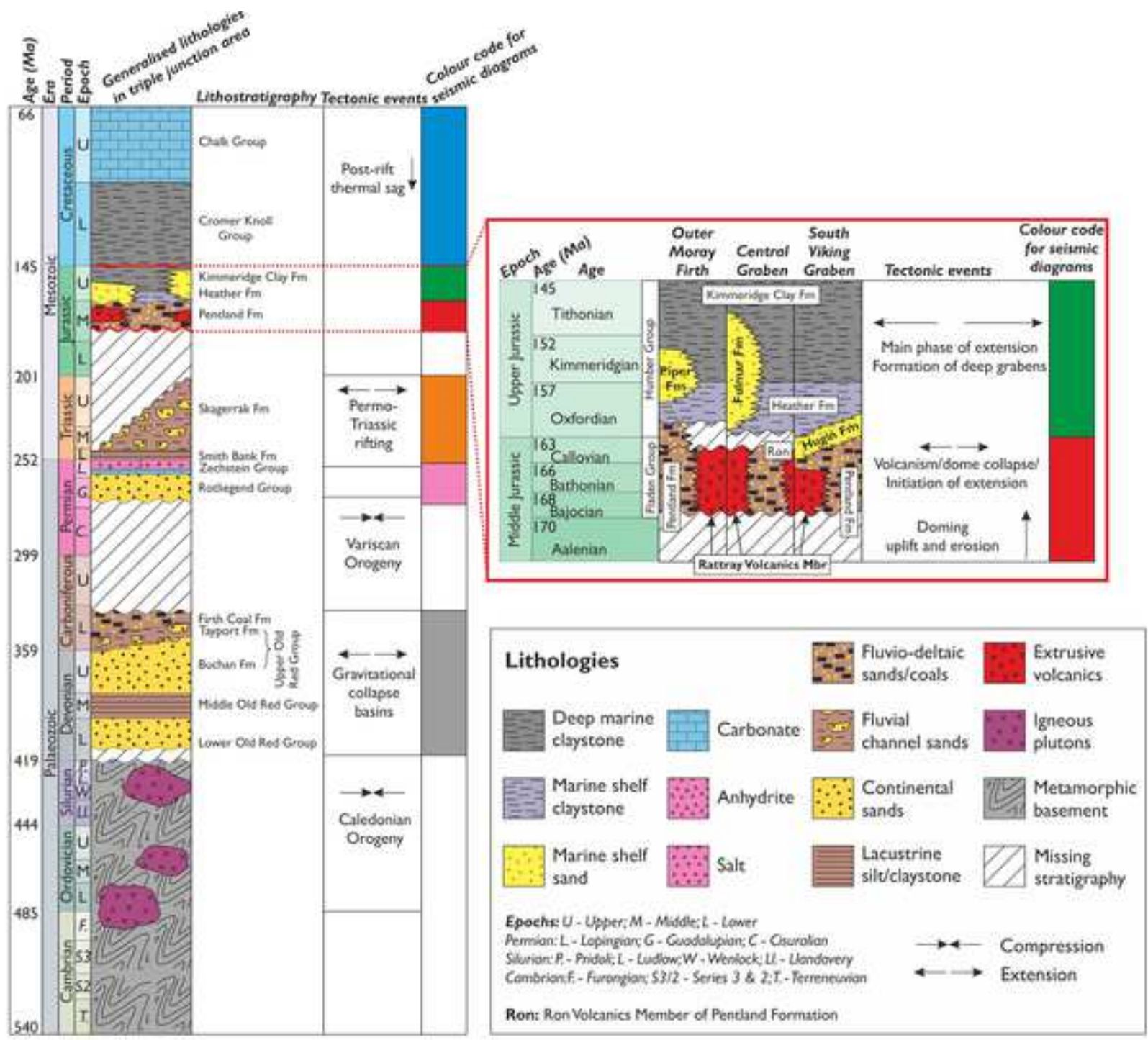
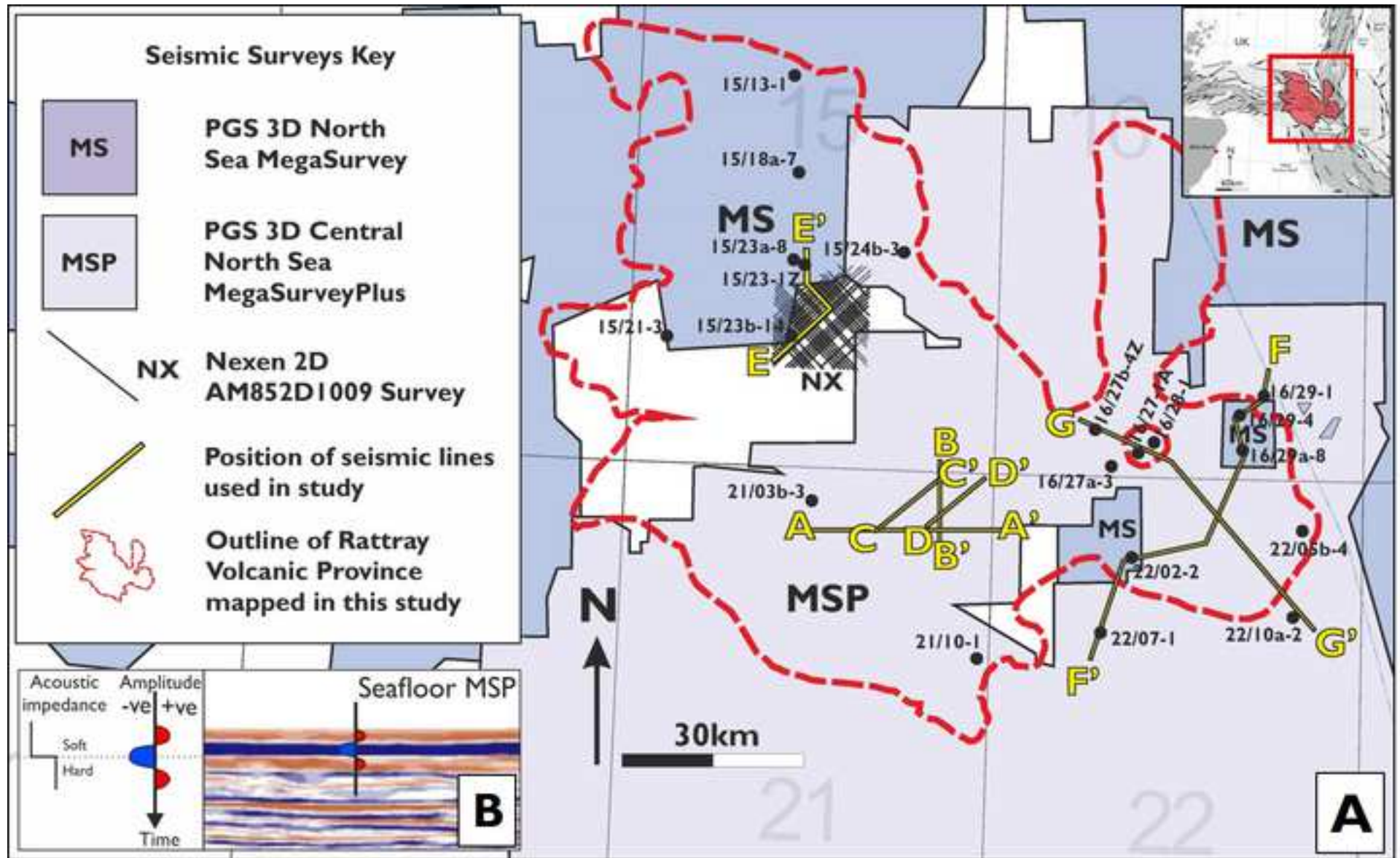
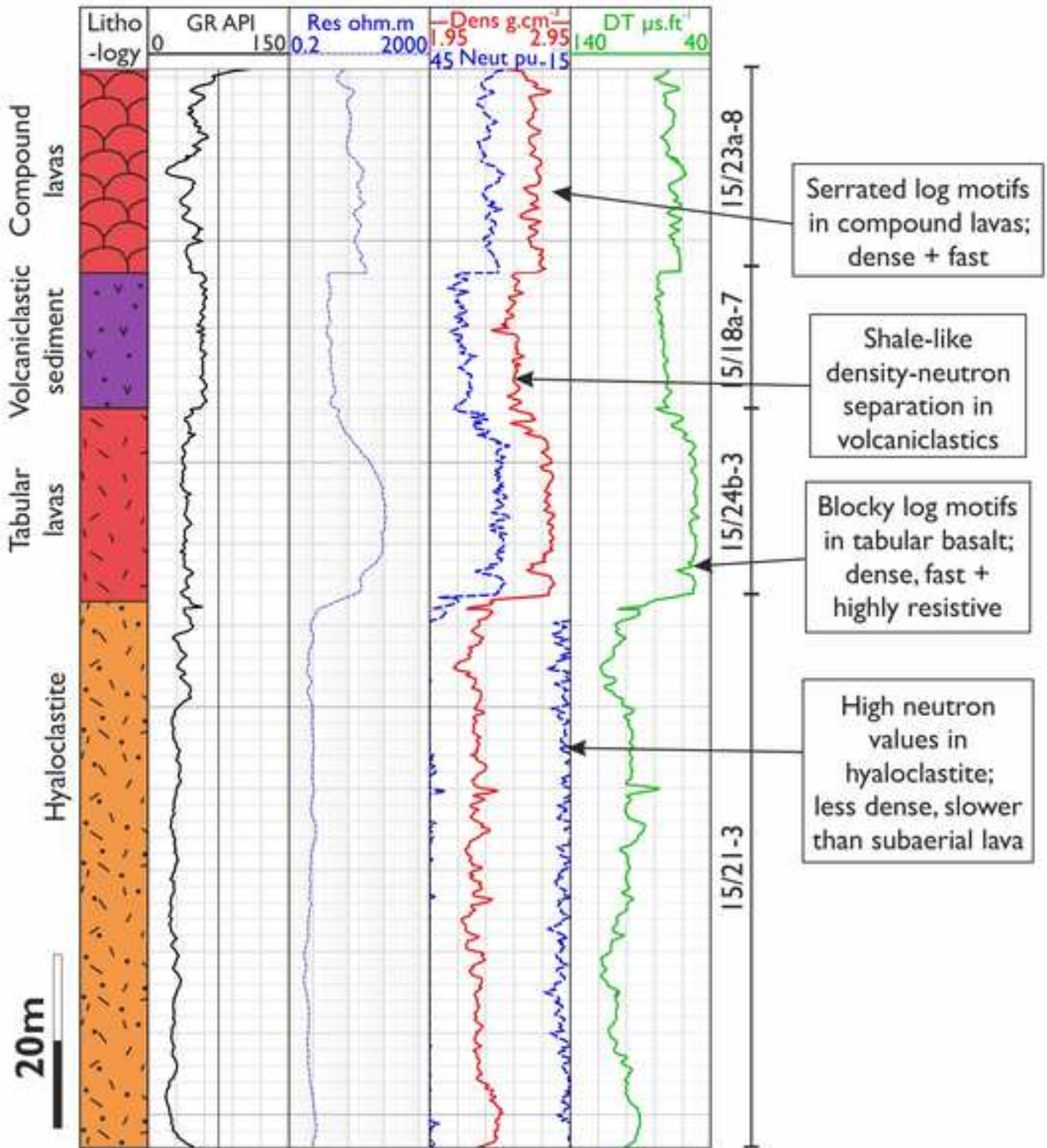
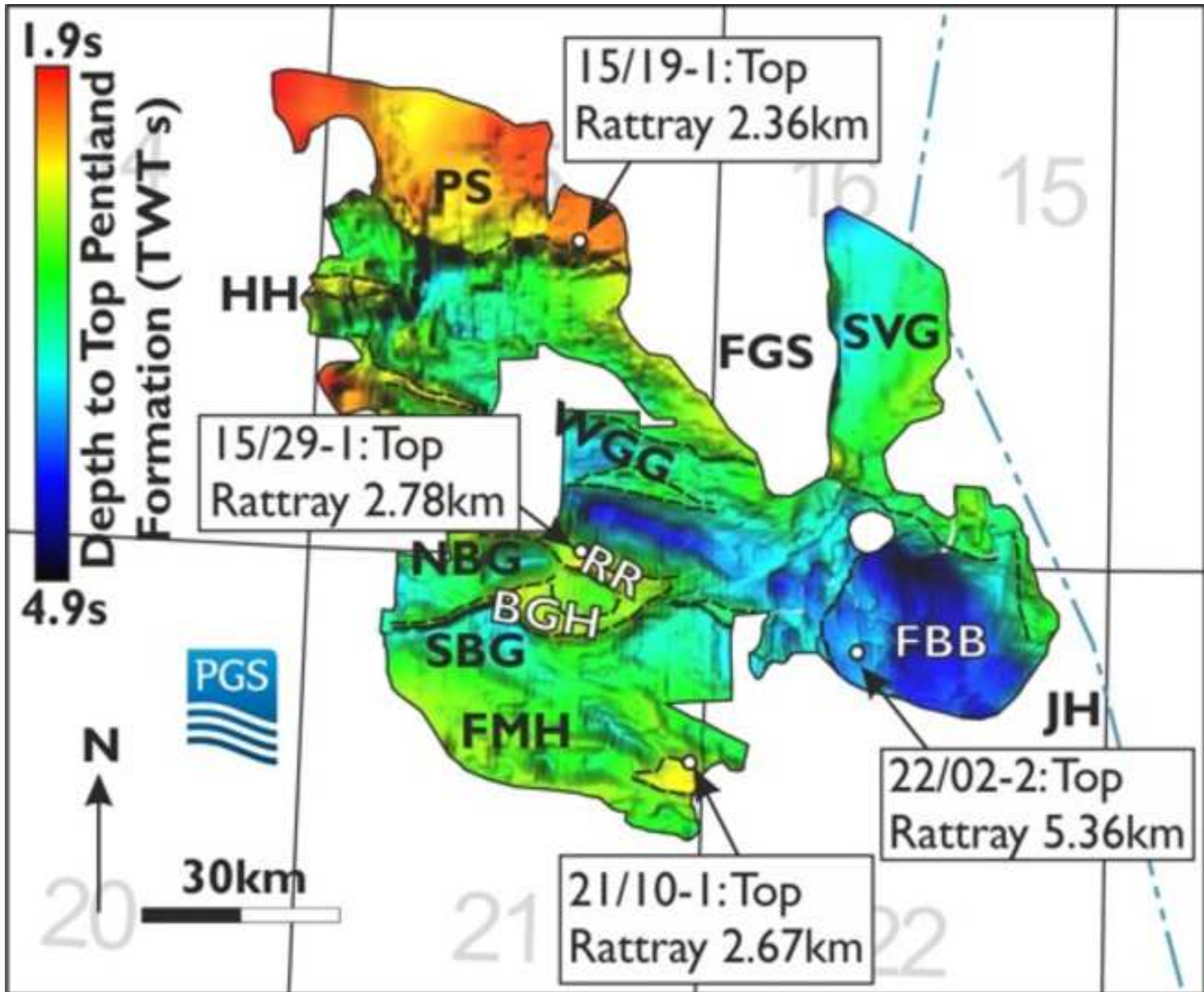


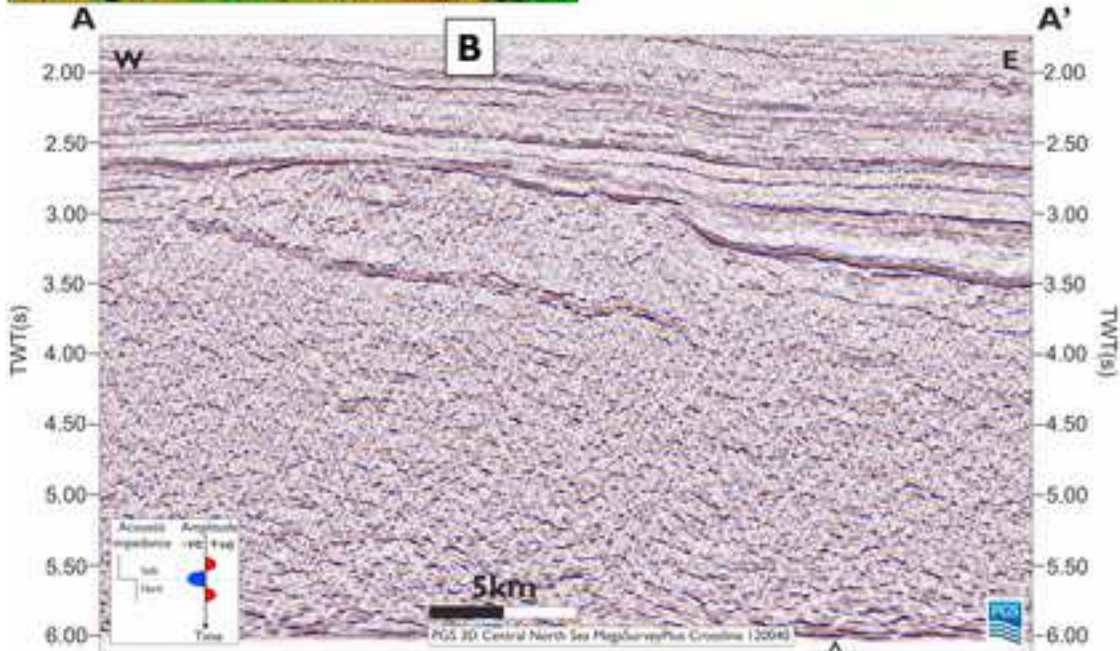
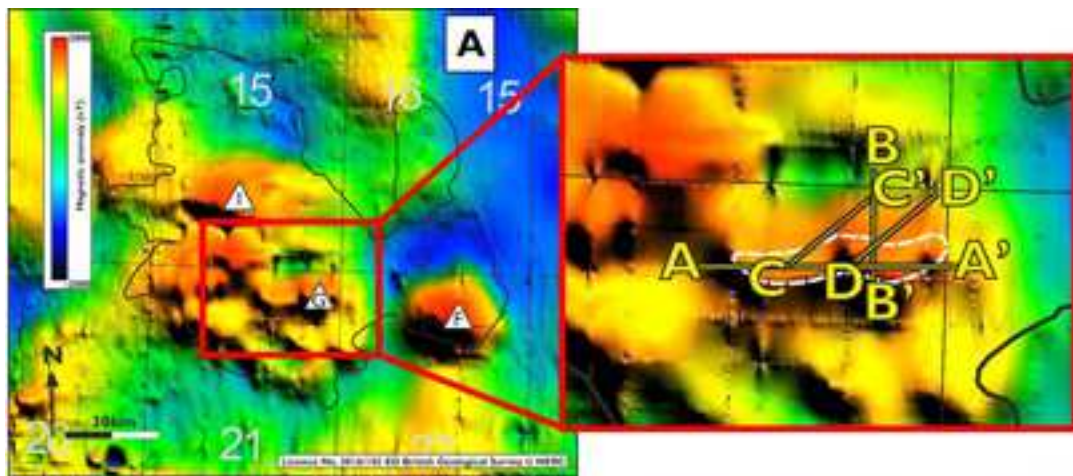
Fig. 2



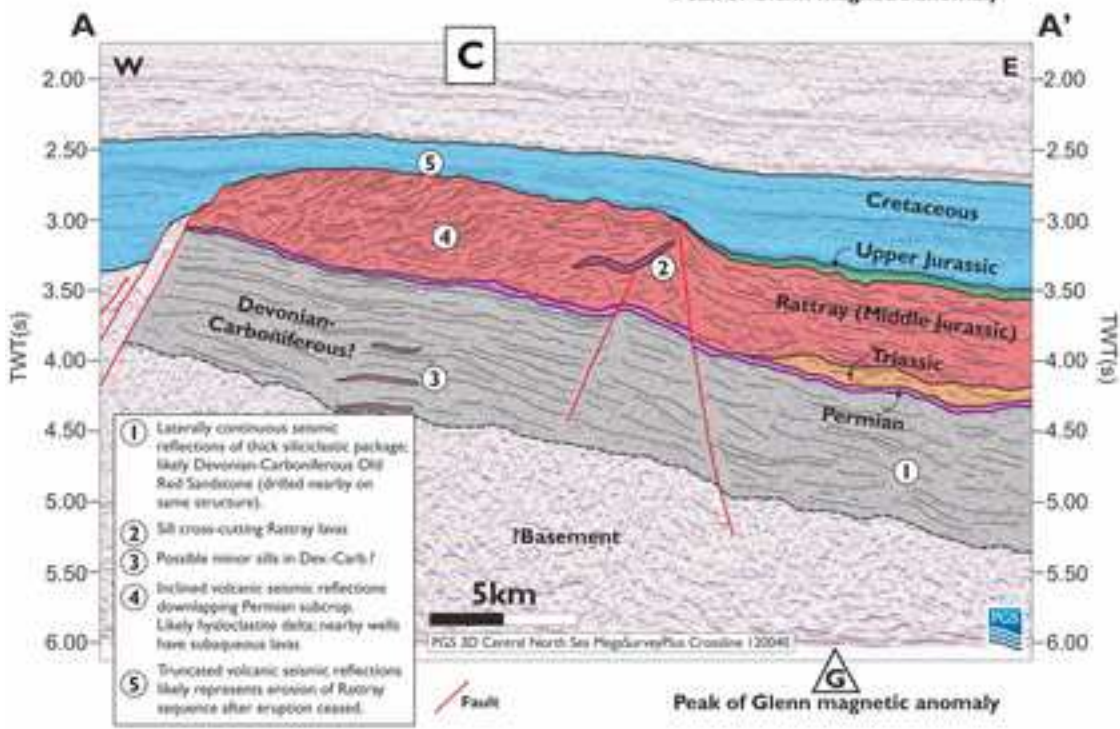




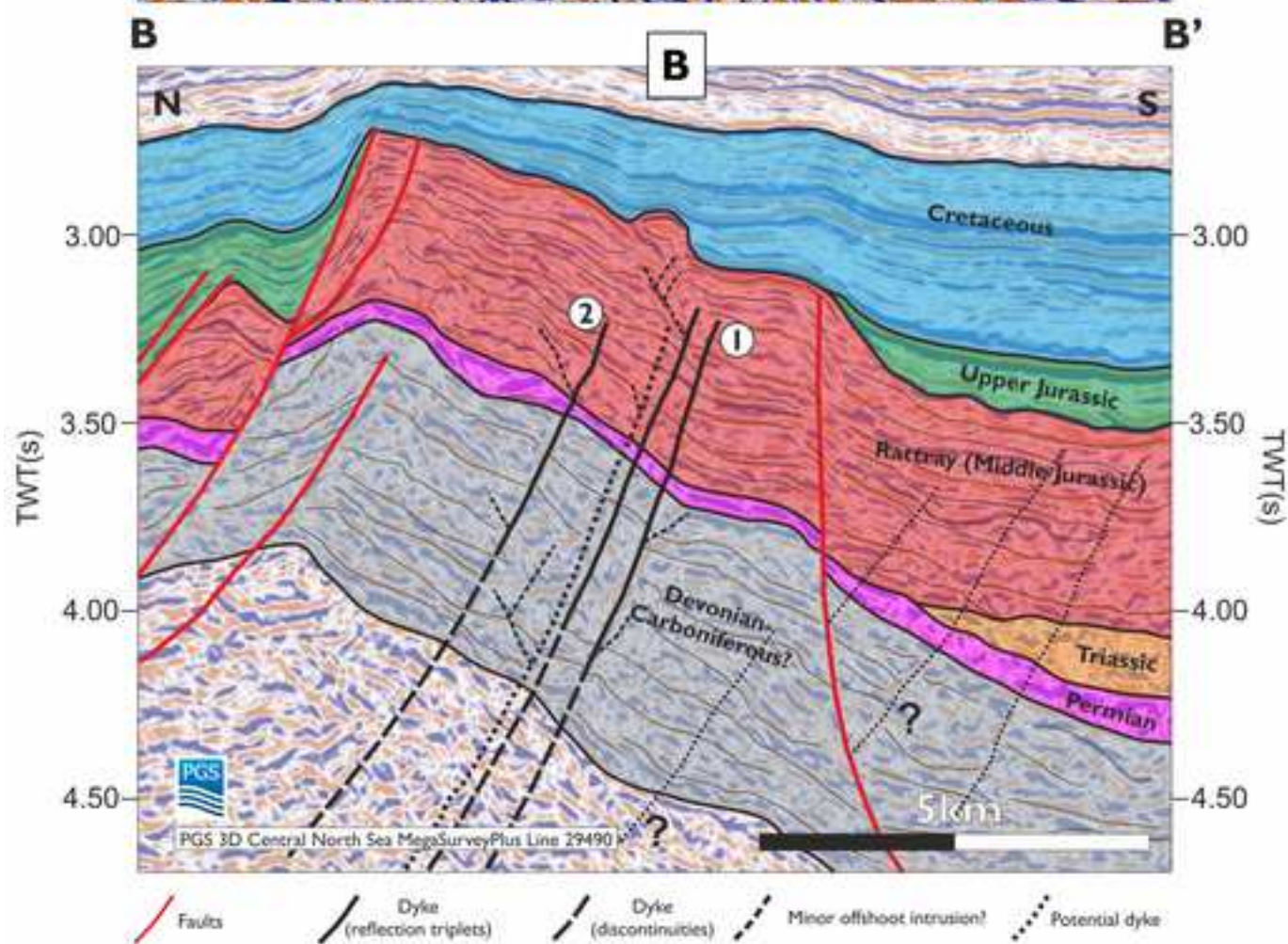
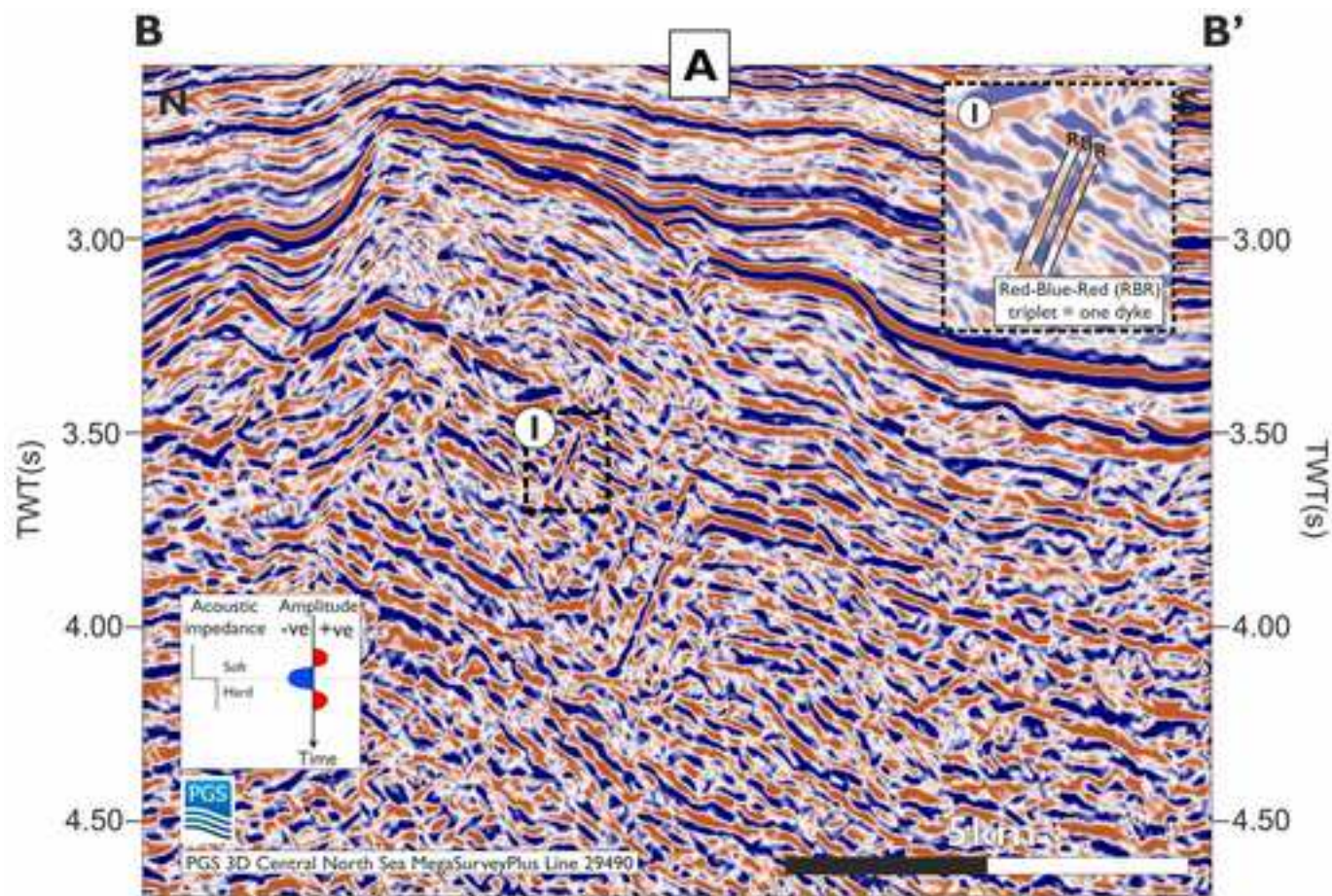


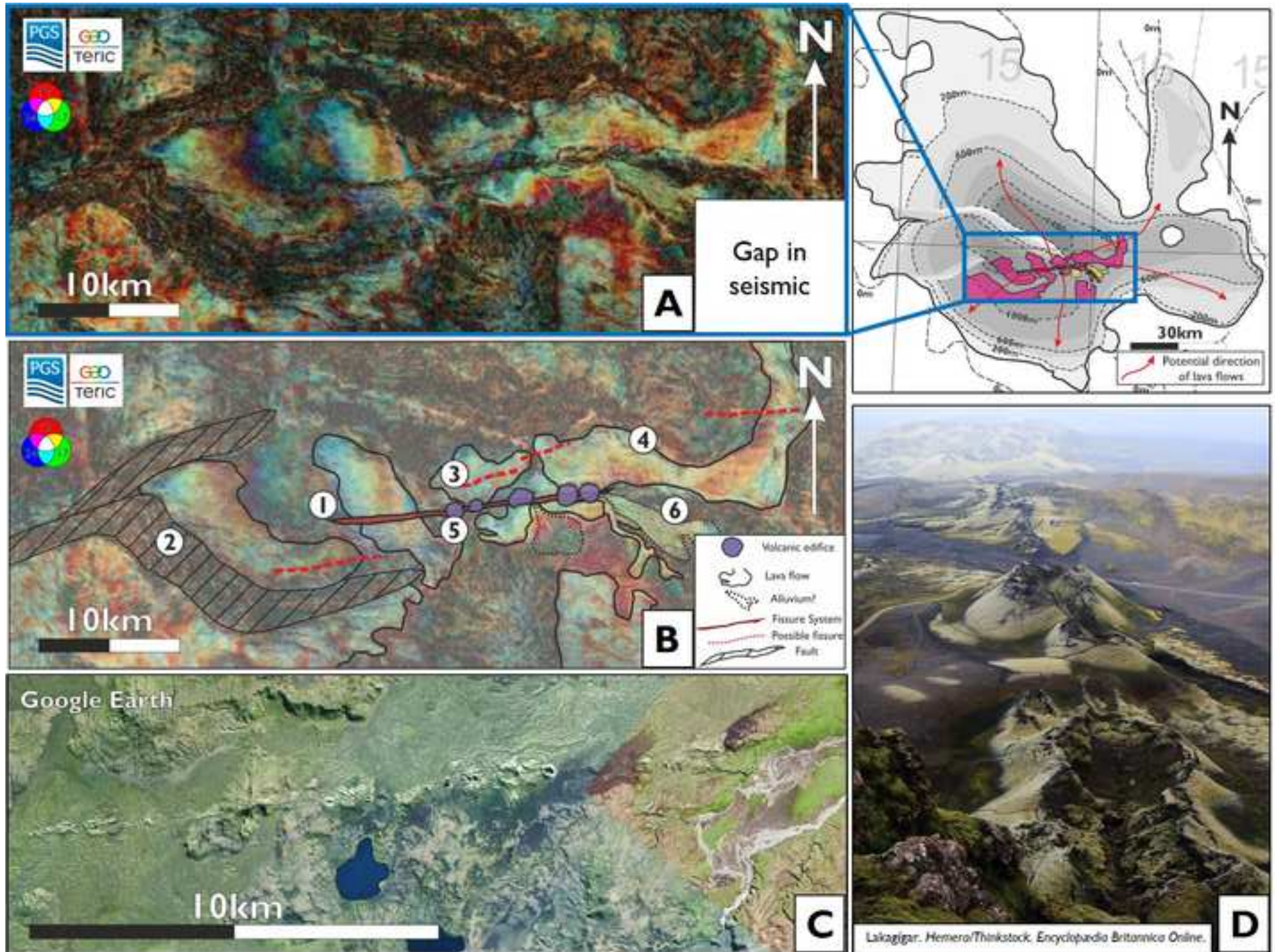


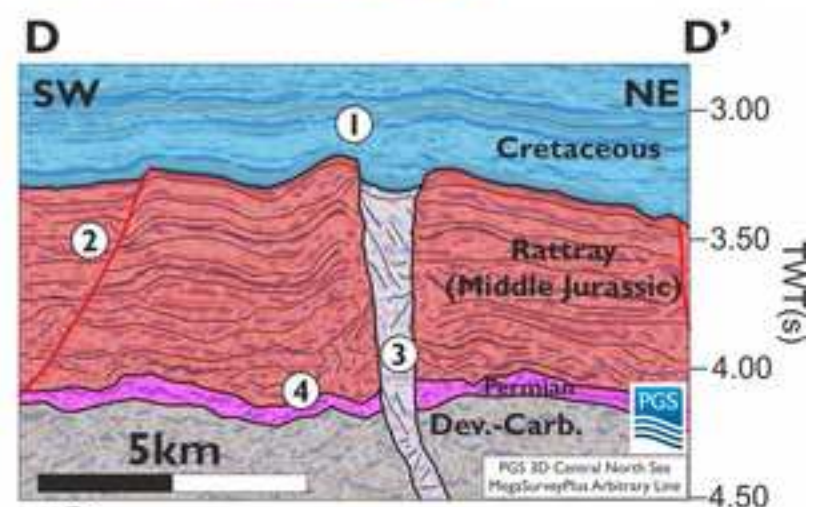
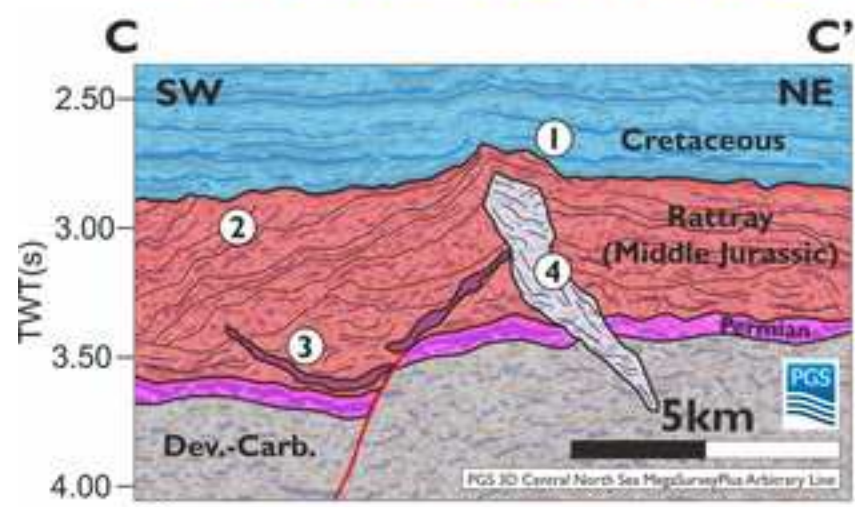
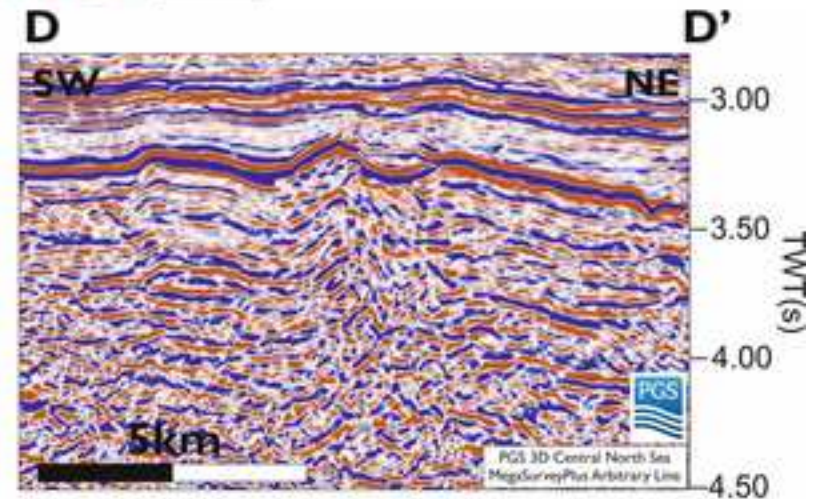
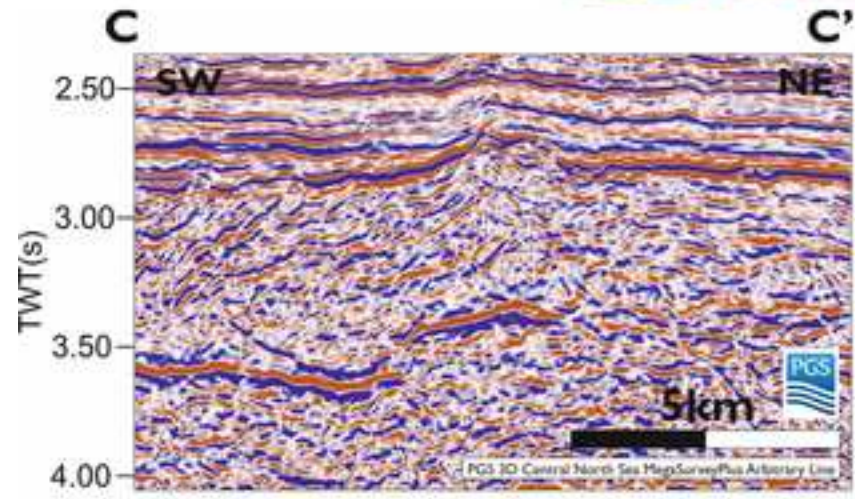
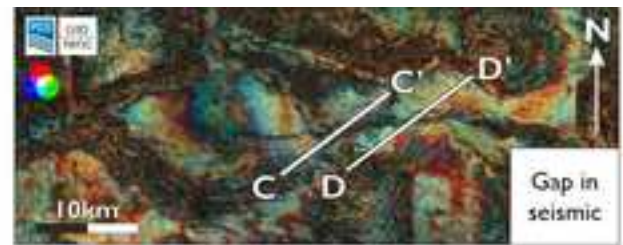
Peak of Glenn magnetic anomaly



Peak of Glenn magnetic anomaly

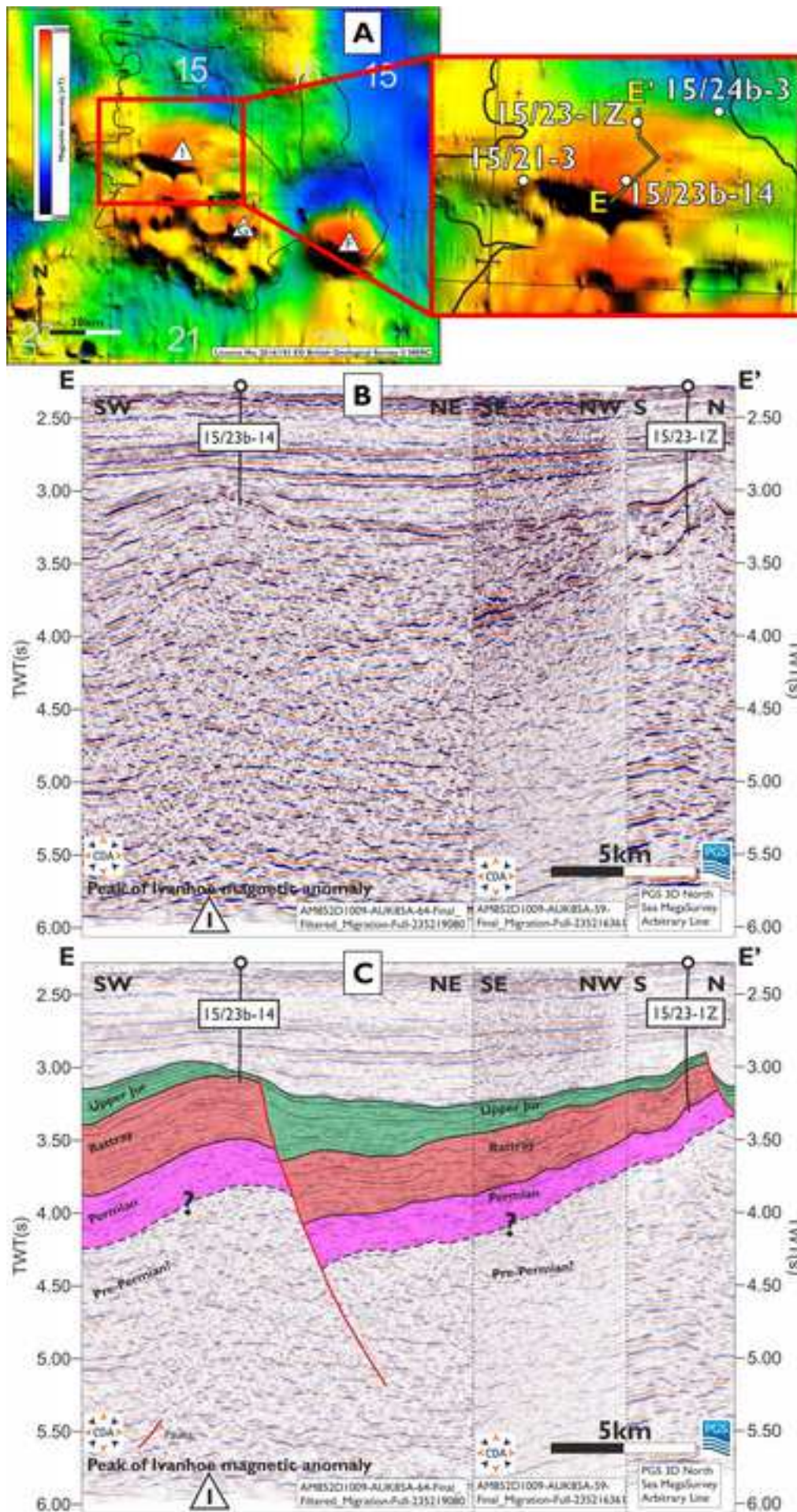


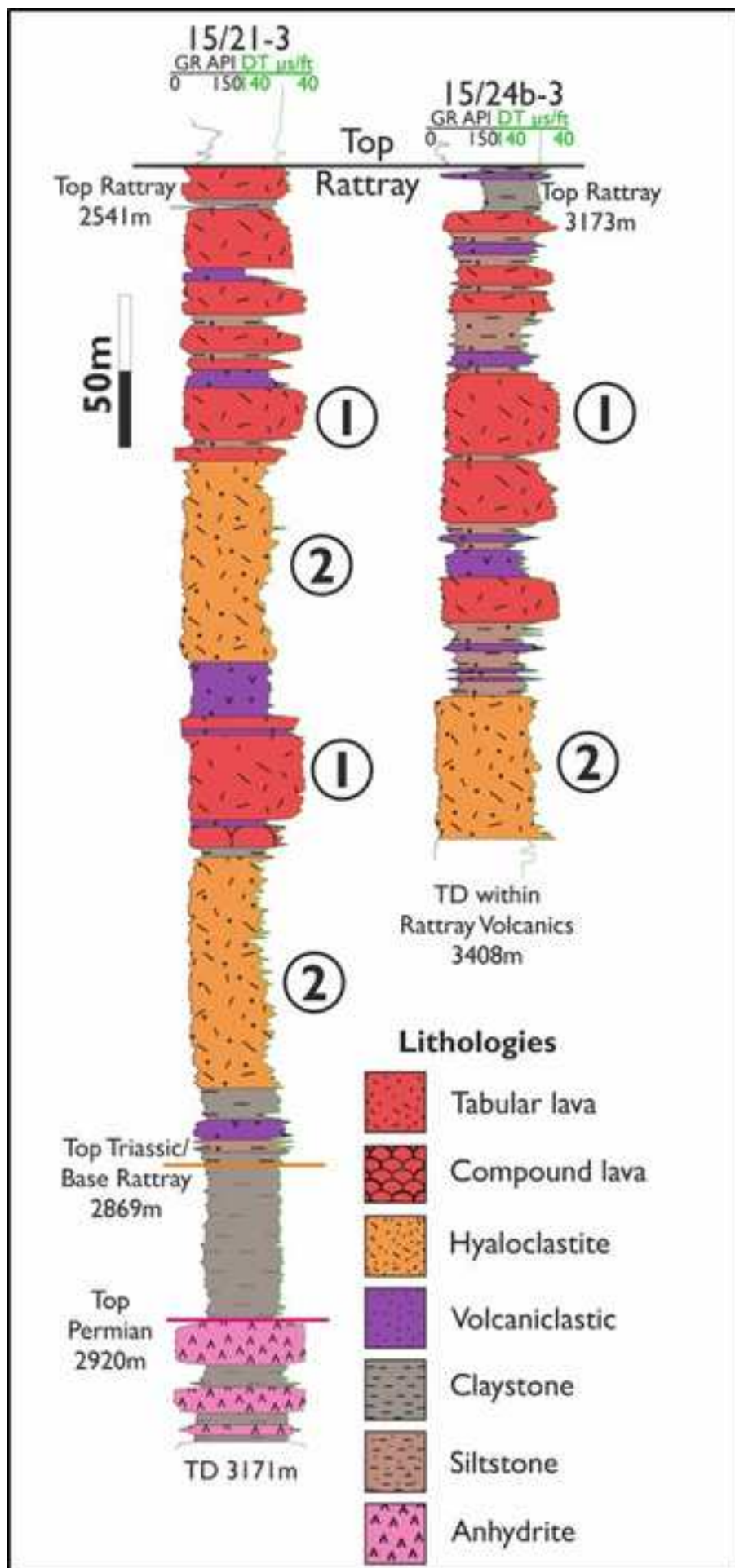


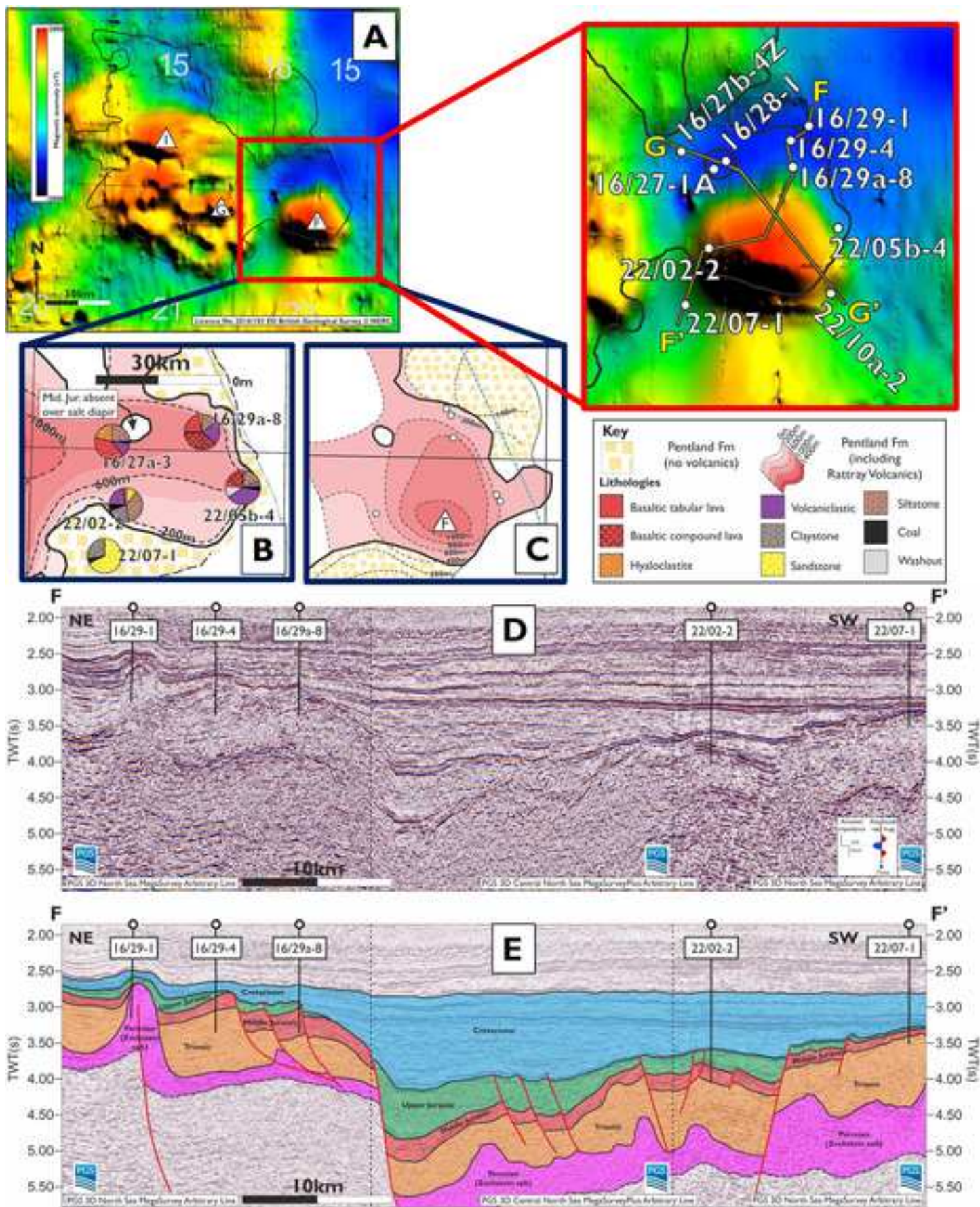


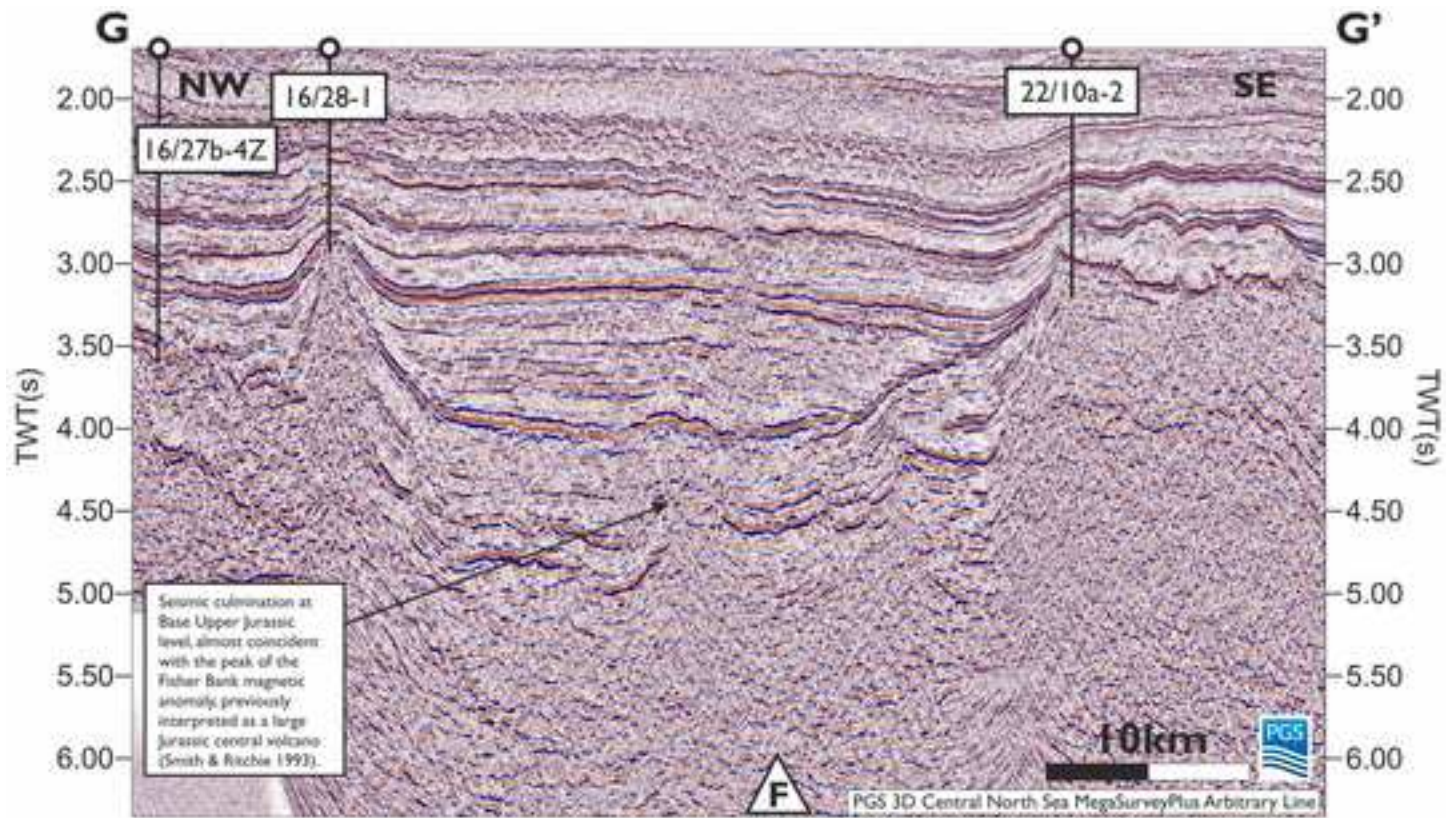
- ① Small volcanic edifice with cinder cone aspect ratio
- ② Truncated inclined volcanic seismic reflections - hyaloclastite?
- ③ Sill intruding Rattray possibly feeding some late stage lavas
- ④ Chaotic seismic reflections within inclined fissure zone beneath vent

- ① Small volcanic edifice above fissure with tuff cone aspect ratio
- ② Laterally continuous volcanic seismic reflections
- ③ Chaotic seismic reflections within fissure zone beneath vent
- ④ Less continuous volcanic seismic reflections - subaqueous lava?

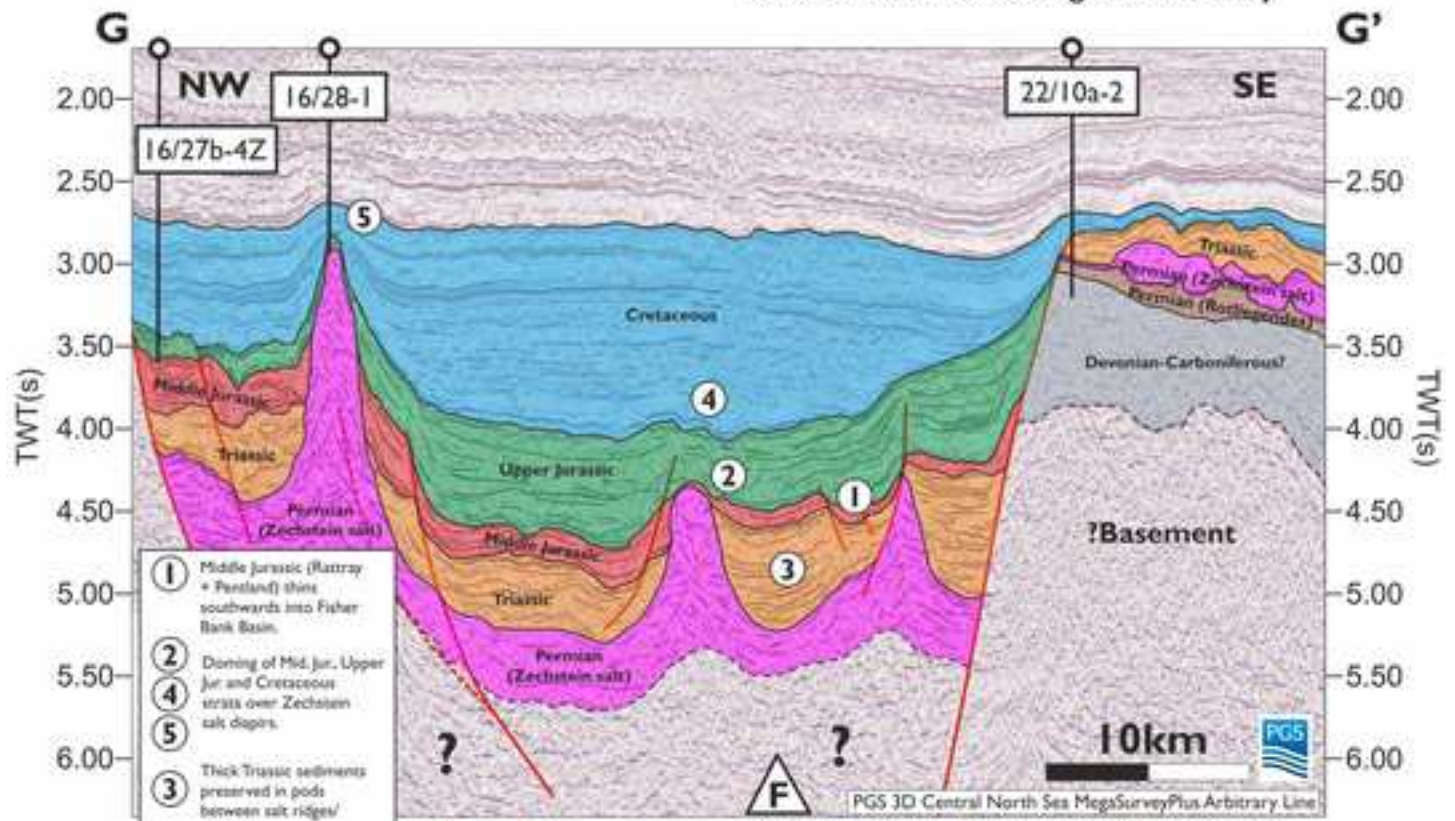




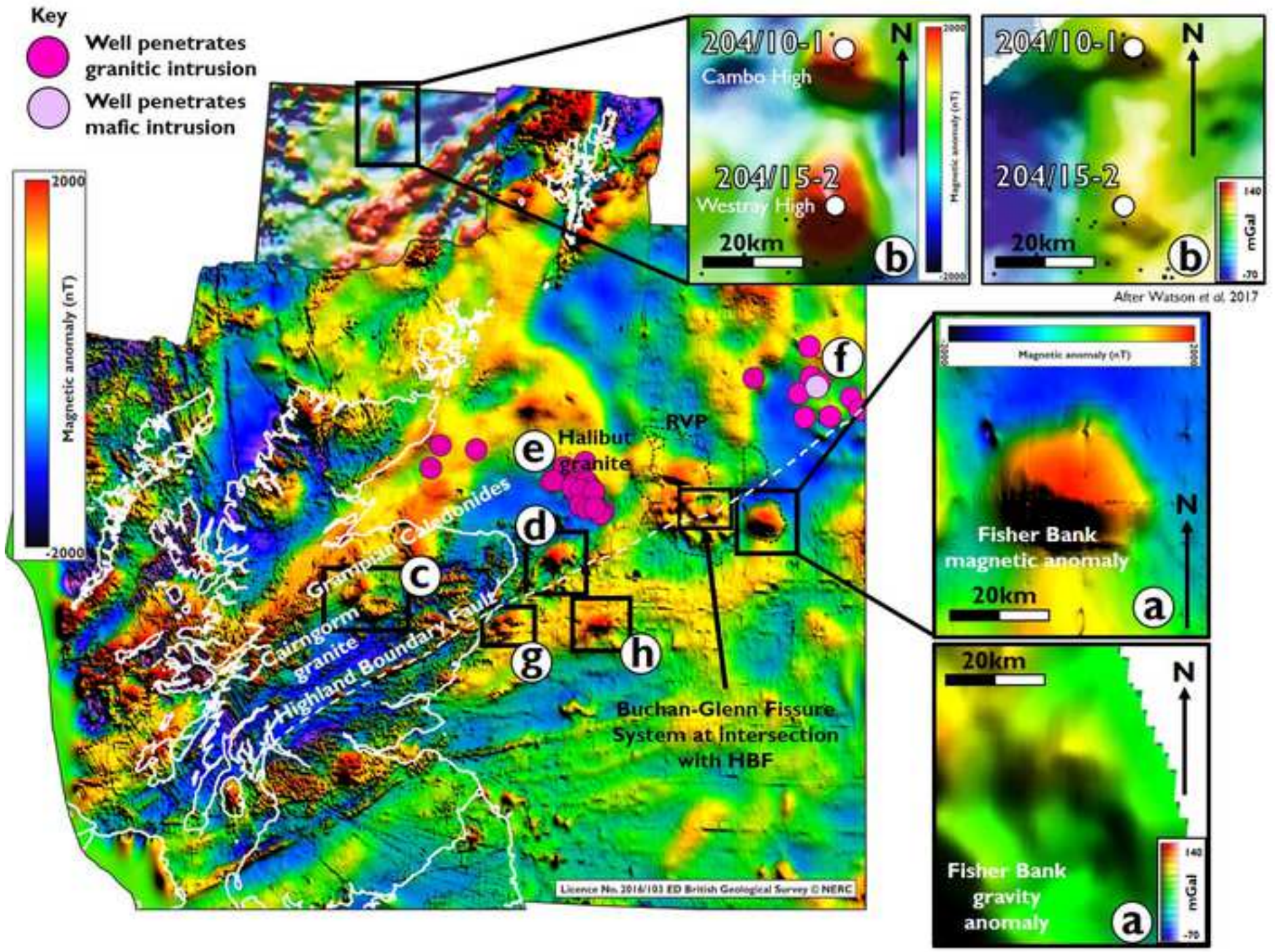




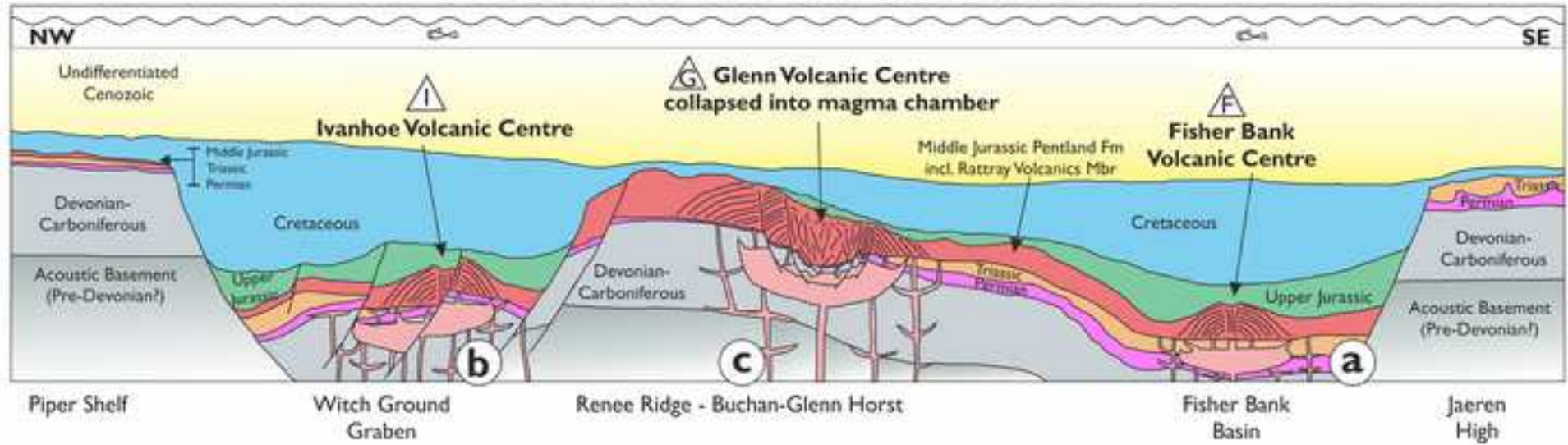
Peak of Fisher Bank magnetic anomaly



Peak of Fisher Bank magnetic anomaly



Previous model: volcanic centres



Revised model: fissure-fed volcanism

